Astron. Astrophys. 327, 825–844 (1997)

ASTRONOMY
AND
ASTROPHYSICS

Chemical reactions in protoplanetary accretion disks

III. The role of ionisation processes

F. Finocchi and H.-P. Gail

Institut für Theoretische Astrophysik, Universität Heidelberg, Tiergartenstraße 15, D-69121 Heidelberg, Germany

Received 21 March 1997 / Accepted 30 June 1997

Abstract. This paper considers the chemistry in a protoplanetary accretion disk during the viscous stage. The model calculation extends our previous work by including in the chemical reaction network the ionisation processes due to cosmic rays and especially the ionisation due to the extinct radio-nuclides ^{26}Al and ^{60}Fe which are known to have been present at the time of formation of our own solar system. We discuss the details of the ionisation by these nuclei and calculate the corresponding ionisation rates. Additionally our model calculation considers the ionisation due to the local radiation field within the disk and it considers the dust destruction processes. We solve the time dependent rate equations for the chemistry simultaneously with equations for a semi-analytic model for the disk structure. The calculation shows that important chemical processes with respect to the chemistry of nitrogen and sulfur are initiated by the ionisation processes and the subsequent ion-molecule reactions which results in substantial amounts of molecular species which would not be formed in a completely neutral chemistry. Especially we find that significant amounts of NH_3 are formed due to ion-molecular reactions in the region where the terrestrial planets are located and that substantial amounts of CS are present in the outer parts of the disk. The C, O, and Si chemistry are found to be not substantially modified by the addition of ionisation processes to the reaction network and our previous results (Finocchi et al. 1997) for the chemistry of these elements are still valid.

Key words: accretion disks – molecular processes – solar system: formation

1. Introduction

The collapse of a rotating molecular cloud leads because of the action of centrifugal forces to a flattened structure: a so called *protostellar disk* revolving around the newly forming star. Some type of viscous process, probably due to turbulent motions, allows the disk material to spiral inwards towards the young central star, while at the same time some portion of the angular momentum is transported outwards. The formation of this *accretion disk* is the widely accepted model to explain the formation of planetary systems.

The evolution of such a disk can approximately be divided into three phases (Cameron 1988):

The first phase of formation is characterised by the rapid infall of matter from the surrounding molecular cloud. In this phase the disk is slowly built up and an embryo of the protostar is present at the center which slowly grows in mass due to direct infall of matter from the molecular cloud and by mass accretion from the disk. This phase lasts for about 10^5 years. In the second phase, the infall of matter from the parent molecular cloud has nearly ceased and most of the mass is concentrated in the central protostar. The protostar slowly grows by continued accretion of mass from the disk. In this *viscous phase* the disk finally has lost most of its former mass to the star, it has become geometrically thin and the temperature in the disk is low, except in its innermost parts close to the star. Some agglomeration processes then can start to operate in the central plane of this *protoplanetary disk* and lead to the formation of planetary bodies. The duration of this phase can be characterised by the viscous time scale, which is about 10^5 years. During the third and last phase (sometimes called the *clearing phase*), the lightest elements composing the disk's matter are dispersed, probably because of the action of a stellar wind from the newly formed star. The heaviest elements can have agglomerated at that time into planetary bodies. If this, indeed, happened, a new planetary system has been born.

In this work, like in our previous contributions (Bauer et al. 1997, Finocchi et al. 1997, hereafter called Paper I and II), we calculate the chemical composition of the disk material in the middle plane of the disk during the second phase (viscous phase) by following a gas parcel drifting form the outer edge of the disk radially to the center under the action of the viscous forces. We neglect a possible continued infall of matter from the surrounding molecular cloud during this phase, which according to observations is likely to occur at a low rate of the order of $< 10^{-7}\, M_\odot/\,\mathrm{yr}$ (van Langenvelde et al. 1994). The calculation

Send offprint requests to: H.-P. Gail (gail@ita.uni-heidelberg.de)

is stopped at about 0.07 AU at the location of the inner one of the two singular points of the disk equations, where a sudden transition to a hot inner disk structure occurs. We perform the calculation in a comoving frame by solving a complex network of chemical reactions coupled with equations for the dust destruction and a semi-analytical model for the disk. A detailed determination of the gas phase chemistry in the disk is necessary to obtain information about the initial conditions in the early phase of our Solar System, about 4.5 Gyr ago.

The present calculation includes the ionisation processes due to cosmic rays and due to the extinct radio nuclides which are known to have been present at the time of formation of our own planetary system. As is well known from astro-chemistry such ionisation processes open reaction channels which are absent in systems where the chemistry evolves by neutral-neutral reactions. We discuss in this paper the influence of these processes on the chemistry in the protoplanetary disk.

The plan of this paper is as follows: The basic equation for the disk's model are briefly presented in Sect. 2. In Sect. 3 we present our basic assumptions for the calculations of the chemistry. In Sect. 4 we discuss the ionisation processes acting in the protoplanetary disk and their ionisation rates. Sect. 5 discusses the initial conditions and in Sect. 6 we present our results, especially the new conclusions with respect to the nitrogen and the sulfur chemistry. The results are summarised in Sect. 7.

2. The accretion disk model

Modeling of the chemistry in a protoplanetary accretion disk requires a knowledge of the run of temperature and total particle density in the midplane of the accretion disk. We determine this from the approximate analytic accretion disk model presented in Duschl et al. (1996)[1] and in Paper I. The basic assumptions of the model are that in the *viscous stage* the disk has relaxed to a quasistationary state for most part of the disk, except perhaps of its inner- and outermost parts and that the disk structure in this stage can be approximated by a thin, non self-gravitating α-disk model. The basic equations for the disk structure in this case are (Duschl et al. 1996)

$$\Sigma = 2500 \frac{\mathrm{g}}{\mathrm{cm}^2} s^{-\frac{3}{5}} \tag{1}$$

$$h = 1.446 \cdot 10^{12}\,\mathrm{cm}\; s^{\frac{21}{20}} \left(\frac{M}{M_\odot}\right)^{-\frac{3}{8}} \left(\dot{M}_{-7}\,\kappa\right)^{\frac{1}{8}} \mu^{-\frac{1}{2}} \tag{2}$$

$$T = 997\,\mathrm{K}\; s^{-\frac{9}{10}} \left(\frac{M}{M_\odot}\right)^{\frac{1}{4}} \left(\dot{M}_{-7}\,\kappa\right)^{\frac{1}{4}} \tag{3}$$

$$P = 71.65 \frac{\mathrm{g}}{\mathrm{cm\ s}^2} s^{-\frac{51}{20}} \left(\frac{M}{M_\odot}\right)^{\frac{5}{8}} \left(\dot{M}_{-7}\kappa\right)^{\frac{1}{8}} \mu^{-\frac{1}{2}} \tag{4}$$

where

$$\dot{M}_{-7} = \frac{\dot{M}}{10^{-7}\,M_\odot/\mathrm{yr}}\,. \tag{5}$$

[1] In the printed version of Duschl et al. (1996) and Paper I the dot over $\dot{M}$ denoting the mass-loss rate is missing in all equations. The correct version may be obtained from the WWW-page of the ITA Heidelberg.

Table 1. Model parameters of the accretion disk used in the computation of disk structure

mass M	$1\,M_\odot$
mass-loss rate $\dot{M}$	$10^{-7}\,M_\odot/\mathrm{yr}$
surface density Σ	2500 g·cm^{-2} at s = 1 AU

s is the radial distance from the protosun in units of AU, Σ is the surface density, h the half thickness of the disk, $M_\odot$ the solar mass, $\dot{M}_{-7}$ the accretion rate through each point of the disk, P and T are the pressure and temperature in the midplane of the disk, κ is the mass extinction coefficient and μ the mean molecular weight. The model parameters of our disk model are summarised in Table 1. They are thought to represent typical values at the time of formation of our own solar system.

The inwards directed drift velocity of the disk material is

$$v_s = 26.94 \frac{\mathrm{cm}}{\mathrm{s}}\, s^{-\frac{2}{5}}\, \dot{M}_{-7}\,. \tag{6}$$

In our calculation of the chemistry in the disk we follow some specific gas parcel as it moves slowly inwards with the drift velocity v_s. The radial distance s of the gas parcel at each instant t can be obtained by integrating (6) with respect to t. It follows

$$s^{1.4} = s_0^{1.4} - 2.52 \cdot 10^{-12} \dot{M}_{-7}\, t\,, \tag{7}$$

where s_0 is the initial position of the parcel at $t = 0$.

In calculating the change of particle density with time in an inwards drifting gas parcel one has to consider that there is a slow vertical velocity component v_z accounting for changes in the disk height as the parcel moves around. The average value of v_z is obviously given by

$$v_z = \frac{dh}{dt} = \frac{dh}{ds}\frac{ds}{dt} = \frac{dh}{ds} v_s\,. \tag{8}$$

Since v_z for symmetry reasons has to vanish at the midplane of the disk, v_z cannot be constant in the vertical direction. In the one zone approximation we can average the vertical gradient of the velocity v_z with respect to the vertical coordinate with the result

$$\frac{\partial v_z}{\partial z} \approx \frac{v_z}{h}\,. \tag{9}$$

The opacity of the disk material is determined self consistently with the temperature. This requires to determine for each time step the zeros of the function

$$F \equiv T - 997 s^{-\frac{9}{10}} \left(\frac{M}{M_\odot}\right)^{\frac{1}{4}} (\dot{M}_{-7})^{\frac{1}{4}} \kappa^{\frac{1}{4}}\,. \tag{10}$$

κ is the Rosseland mean of the total mass extinction coefficient (gas and dust) which depends on the temperature. For the opacity of the gaseous component of the disk material we use the analytical expressions given by Lin and Papaloizou (1985) and Bell and Lin (1994). Three different approximations are used

for this opacity depending on the dominating absorbing species. If molecules dominate the extinction, the mass extinction κ is approximated by

$$\kappa_{\rm mol} = 1.0\,10^{-8} \cdot \rho^{\frac{2}{3}} \cdot T^3 \quad {\rm cm}^2/{\rm g}\,, \tag{11}$$

where ρ is the gas density. If H^- dominates the extinction, we use

$$\kappa_{\rm H^-} = 1.0\,10^{-36} \cdot \rho^{\frac{1}{3}} \cdot T^{10} \quad {\rm cm}^2/{\rm g}\,, \tag{12}$$

and if atomic and ionic *bf*- and *ff*-transitions dominate, we use

$$\kappa_{\rm bf} = 1.0\,10^{20} \cdot \rho \cdot T^{-\frac{5}{2}} \quad {\rm cm}^2/{\rm g}\,. \tag{13}$$

In order to calculate the total gas opacity, we use the following interpolation formula

$$\frac{1}{\kappa_{\rm gas}} = \frac{1}{\kappa_{\rm mol} + \kappa_{\rm H^-}} + \frac{1}{\kappa_{\rm bf}}\,, \tag{14}$$

which smoothly interpolates between the different opacity regions (see Fig. 1 in Paper II).

The Rosseland mean of the dust opacity is calculated from the dust absorption model of Draine and Lee (1984) and Draine (1985). The total mass extinction finally is calculated from

$$\kappa = \kappa_{\rm gas} + \kappa_{\rm dust} = \kappa_{\rm gas} + \frac{\rho_s}{\rho}\kappa_s + \frac{\rho_c}{\rho}\kappa_c\,. \tag{15}$$

This linear superposition of opacities should be of sufficient accuracy for our model. ρ_s and ρ_c are the mass density of the carbon and silicon dust in the gas-dust mixture (which goes to zero as the dust is destroyed!). κ_s and κ_c are their respective extinction coefficients.

A special property of the Eqs. (1) ... (4) for the structure of stationary accretion disks, in combination with the strong temperature dependence of the opacity in certain temperature regions, is the existence of two singular radii s, at which the derivative of T with respect to s becomes infinite (cf. Fig. 2 of Paper II). Between these critical radii the nonlinear system of equations for the disk structure has a threefold solution for $T(s)$ for which two solution branches each merge in the singular points. Of these three solutions the two branches corresponding to the lowest and the highest temperature are stable, while the middle branch represents an unstable solution which evolves towards one of the two stable solutions if perturbed.

A consequence of this special structure of the solution is that any solution for the disk structure extending from close to the star out to very large distances cannot be continuous everywhere. There necessarily exists a discontinuous temperature jump somewhere between the two singular radii. The position of this jump cannot be specified within the frame of the stationary disk model. In time dependent models this singular behaviour of the stationary solution results in the well known phenomenon of running ionisation fronts, which are responsible for the phenomenon of dwarf novae outburst in accretion disks around compact objects (see, e.g., the review by Cannizzo 1993) and they are most likely responsible for the FU Ori phenomenon connected with protoplanetary disks during the infall phase (see, e.g., Hartmann and Kenyon 1996 for a review). Here we are interested in the viscous phase of the accretion disk where FU Ori type outburst are not likely to occur (Bell et al. 1995). It may, however, be that small fluctuations observed for some T Tauri objects (Herbig 1977) may be related to such running waves in the region between the singular points of the stationary solution (Hartmann and Kenyon 1996).

In our model calculation we arbitraryly assume that the discontinuous jump from the low temperature branch of the solution to the high temperature branch occurs at the inner singular point which is located at $s = 0.0728\,{\rm AU}$ for our choice of model parameters. The outer singular point is located at $s = 0.186\,{\rm AU}$. Our solution for the disk structure and the chemistry of the disk material, then, strictly speaking only applies to the region $s > 0.186\,{\rm AU}$. Within the radius regime $0.186\,{\rm AU} < s < 0.0728\,{\rm AU}$ the actual disk structure depends on the history of the disk evolution and should in principle be calculated from time dependent models.

The equations for the disk structure do not consider the possibility of infall of matter from the surrounding molecular cloud onto the disk. Though there are strong indications that there exists continued infall even in the T Tauri phase this infall is likely to be concentrated to the outer parts of the disk (cf. Cassen (1994), appendix A) which are not considered in our calculation.

3. Chemistry in the disk

3.1. Basic equations

In order to determine the chemical composition of the disk at each radius, we perform, as in our previous work (Papers I and II), a fully kinetical treatment of all the possible chemical reaction pathways. This is necessary because the densities and temperatures in most parts of the disk are much too low to allow the system to evolve into chemical equilibrium. In the warm inner part of the accretion disk, however, the densities and temperatures are much higher and the unfreezing of a lot of reaction paths, which are kinetically inhibited in the cold outer disk, drives the chemistry towards an equilibrium state. We do not take recourse to the simplified treatment of the chemistry possible for these warm inner parts of the accretion disk but we will consider explicitly the reaction kinetics in the whole disk from the cold outer parts down to the hot central part.

We consider in this calculation two-body reactions between atomic and molecular species from the gas phase and two three-body reactions between atomic and molecular hydrogen. The ternary reactions between H and H_2 are relevant in our problem because the system evolves very slowly and therefore a long time scale is available for molecule formation. The time evolution of a specific species is governed by the continuity equation

$$\frac{\partial n_i}{\partial t} + \nabla \cdot (n_i \boldsymbol{v}) = 0\,, \tag{16}$$

where $\boldsymbol{v}$ is the velocity of matter and n_i is the particle density of the species under consideration. If we use a cylindrical coordinate system, we get for the change of n_i along a streamline

$$\frac{\mathrm{d}n_i}{\mathrm{d}t} = \frac{\partial n_i}{\partial t} + v_s \frac{\partial n_i}{\partial s} + v_z \frac{\partial n_i}{\partial z} \,. \tag{17}$$

z is here the vertical height over the midplane. We have assumed rotational symmetry of the disk in the azimuthal direction. The addition of the source terms to the continuity equation provides an ordinary differential equation for n_i in the comoving frame

$$\begin{aligned} \frac{\mathrm{d}n_i}{\mathrm{d}t} \;=\; & -n_i \left(\frac{v_s}{s} + \frac{\partial v_s}{\partial s} + \frac{\partial v_z}{\partial z} \right) \\ & -n_i \sum_j k_{ij} \cdot n_j + \sum_{jl} k_{ijl} \cdot n_j \cdot n_l \\ & -n_i \sum_{jl} k_{ijl} \cdot n_j \cdot n_l + \sum_{jlm} k_{ijlm} \cdot n_j \cdot n_l \cdot n_m \,. \end{aligned} \tag{18}$$

k_{ij}, k_{ijl}, and k_{ijlm} are the rate coefficients of the reactions. They are approximated by the Arrhenius law

$$k = k_0 T^{\alpha} \exp\left(-\frac{E_a}{kT} \right) \,. \tag{19}$$

k_0 and α are constants, k is the Boltzmann constant and E_a is the activation energy barrier.

The system of ordinary differential equations, one for each species present in the system, must be solved together with Eqs. (3), (4) and (7) determining at each instant the temperature and pressure in some gas parcel and its radial distance from the protostar. Inspection of Eqs. (3) and (4) shows that the temperature and the opacity must be calculated self consistently with the chemistry (see Papers I and II).

3.2. The chemical reaction network

The chemical reactions network for neutral-neutral reactions is the same as that used in Papers I and II, i.e., we use for the HCON chemistry the reaction network given by Mitchell (1984). This system has been extended and updated by some reactions given in Baulch et al. (1992). Improved rate coefficients for the reactions

$$C_2H_3 + H_2 \rightarrow H + C_2H_4 \tag{20}$$

and

$$C_2H_3 + H \rightarrow H_2 + C_2H_2 \tag{21}$$

have been included, too (Romani 1996). The silicon chemistry is taken from Britten et al. (1990). This chemistry is extended by some reactions given in Millar et al. (1991)[2]. For the sulfur chemistry we have taken the reaction network given by Millar et al. (1991).

[2] We used the updated version of the list of reactions rates obtained from the WWW.

The whole reaction network for the ion chemistry is taken from Millar et al. (1991). Recombination rate coefficients for ions not listed in Millar et al. (1991) are taken from Landini and Monsignori Fossi (1990). This chemistry includes all the ions than can be formed with H, C, O, N, Si, and S. Additionally, we consider the atoms and ions of Na, Ca, Al, and Ca since these are important electron donators when thermal ionisation in the dense warm inner part of the disk starts to become important.

Finally, we have added to the r.h.s. of the system of rate equations (18) the ionisation rates for H_2 and He due to the ever present cosmic rays as calculated by Umebayashi and Nakano (1981) for the specific conditions encountered in protoplanetary disks (see Sect. 4.1), the ionisation rates by long lived unstable radio nuclides (see Sect. 4.2), and the ionisation rates for thermal ionisation in the inner parts of the disk (see Sect. 4.3).

We have to deal now with a system of 156 species (atoms, molecules, ions and electrons), i.e., 156 differential equations coupled by a network of more than 1200 chemical reactions. The radius changes of the different kinds of dust particles considered in the model (troilite, graphite and olivine) adds three additional differential equations to the system. The self consistent determination of the disk structure and temperature and of the opacity and its changes due temperature changes and dust destruction provides a set of algebraic equations coupled to the system of differential equations. This changes the mathematical nature of the problem from solving a system of ordinary differential equations to that of solving a system of differential-algebraic equations. The size and particular the stiffness of our chemical system requires the use of a powerful integrator. DAESOL (Bleser 1986, Eich 1987, Bauer 1994) in our previous calculations (Papers I and II) turned out to be a very powerful tool for this kind of problems and has also been used in this calculation. Details about the code can be found in Paper I.

3.3. The dust model

A detailed description of the ice and dust models used in this work can be found in Papers I and II. We remind here the main features of our models:

a) Only CO and H_2O are present as ices in our model. These species are supposed to form coatings on the dust grains. Because CO and H_2O have different sublimation temperatures (resp. $\approx$25 K and $\approx$150 K), we separate the H_2O and the CO ices in two distinct layers. CO because of its lower sublimation temperature should be the outer one. Other ice species are known to be present (like CH_3OH and NH_3, see Pollack et al. 1994) but they have a too low abundance and we will neglect them.

b) Three dust components are assumed to be present in the disk's matter: olivine (Mg_2SiO_4), carbon dust (graphite) and troilite (FeS). Silicate dust (olivine) is destroyed by thermal decomposition at about 1 650 K. We assume the following destruction process

$$Mg_2SiO_4\,(\mathrm{solid}) \quad \longrightarrow \quad 2Mg \;+\; SiO \;+\; 3O \,. \tag{22}$$

Table 2. Solar system abundances of the heavy elements relative to Si (Anders and Grevesse 1989, Grevesse and Noels 1993)

Element		ϵ / $\epsilon_{\rm Si}$
Aluminium	Al	$8.49 \cdot 10^{-2}$
Calcium	Ca	$6.11 \cdot 10^{-2}$
Natrium	Na	$5.74 \cdot 10^{-2}$
Kalium	K	$3.77 \cdot 10^{-3}$

The details are outlined in Paper I. This pure vapourisation process yields a slightly higher temperature for dust destruction than calculations of chemical equilibrium between this solid and the gas phase predicts for the disappearance of this dust component for a mixture of elements with cosmic abundances (e.g. Grossman 1972). This difference is due to the fact that chemical equilibrium calculations in a hydrogen rich environment requires a net reaction scheme of the form

$$\mathrm{Mg_2SiO_4\,(solid)\ +\ 3H_2\ \longrightarrow\ 2Mg\ +\ SiO\ +\ 3H_2O} \quad (23)$$

since no free O atoms exist in a chemical equilibrium state at the relevant pressures and temperatures. The reaction enthalpies of the two reactions are different by the enthalpy of formation of H_2O from O and H_2. This leads to different destruction temperatures of the solid. Our assumption of a pure thermal decomposition (22) supposes that chemical sputtering of silicates by hydrogen is kinetically forbidden.

Our calculation of the thermal ionisation requires to consider the less abundant but readily ionisable elements Na, Ca, Al, and K as electron donators. The two elements Ca and Al are completely condensed into the dust grains, as is indicated by their very high degree of depletion from the interstellar gas (e.g. Jenkins 1989, Cowie and Songaila 1986). The two alkali metals Na and K are much less depleted, but also for these two elements the major part seems to be built into the dust (e.g. Jenkins 1989). For simplicity we assume in this paper that Na and K are completely condensed into grains. These elements, then, are injected into the gas phase during the destruction of the dust. We do not consider the details of this process and especially we do not consider that Al and Ca probably form some Ca-Al-Silicate which persist to much higher temperature than the Mg-Fe silicates. We simply assume that Na, Ca, Al, and K are released from the grains while the silicate dust component vapourises. Their injection rate into the gas phase is approximated by the injection rate of SiO during silicate decomposition times their abundance ratio to Si. The element abundances of these elements used for this calculation are shown in Table 2.

As explained in Paper II, carbon dust is mainly destroyed by oxidation processes (chemical sputtering). The most efficient oxygen bearing species in the gas phase of an accretion disk for the oxidation of carbon are OH and O (In the earth's atmosphere the molecular oxygen O_2 would be the most important species for carbon oxidation). The pure sublimation of this dust with injection of free carbon atoms or molecules into the gas phase does occur but it is absolutely inefficient compared with the oxidation processes.

Troilite converts at about 700 K into Fe and S. For computational simplicity we treat this process as the decomposition

$$\mathrm{FeS\,(solid)\ \longrightarrow\ Fe\ +\ S}\,. \quad (24)$$

As argumented in Paper II, we suppose that 50 % of the available sulfur is locked in the troilite particles. The remaining 50 % must be present in the gas phase or is frozen into the ice coatings of the dust grains. By passing the accretion shock the ice coatings of the grains vapourise and the sulfur bearing ices components likely to exist in the parent molecular cloud (SO, SO_2, H_2S) should sublimate and they will quickly react to form H_2S. For that reason we suppose that the remaining 50 % of the sulfur are bound in hydrogen sulfide.

The ensemble of dust particles including the ice layers is assumed to have their sizes distributed according to MRN size distribution (Mathis et al. 1977)

$$f(a)da = Ca^{-\frac{7}{2}}da\,. \quad (25)$$

a is the particle radius and C is a constant ($\log C = -15.14$ for silicate dust and $\log C = -15.20$ for carbon dust). According to the findings of Mathis et al. we assume that 70 % of the available carbon is locked in carbon grains and the remaining fraction of 30 % is supposed to be present as CO (ice). The silicate is assumed to be completely condensed into olivine.

4. Ionisation processes

In our previous calculations (Paper I and II) we have neglected the influence of ionisation processes on the chemical processes. In the present work we include three possible sources of ionisation already mentioned in our previous papers: the ionisation due to the ever present cosmic rays, to the extinct radio nuclides like ^{26}Al or ^{129}I, which are known to have existed in the early phases of our Solar System, and we perform an LTE calculation for the ionisation by UV photons.

4.1. Ionisation by cosmic rays

An important source of ionisation are the ever present cosmic rays. They are the dominant sources of ionisation in molecular clouds (Spitzer and Tamasko 1968, see also Dalgarno and McCray 1972) and the ionisation rate has been determined several times for conditions valid for such clouds (see the short review by Lepp(1992)). In the protoplanetary disk case the mass surface density, contrary to interstellar molecular clouds, is very high and most of the cosmic ray particles cannot easely cross the disk material but are completely stopped within the disk. Then, cascade effects and ionisation due to secondary particles becomes very important. This problem has been considered in some detail by Umebayashi and Nakano (1981) for the solar nebula problem. They considered the particle production and energy loss processes and solved the corresponding particle transport equations for the plane parallel slab problem and determined

the resulting ionisation rate. We use in our model calculation their results for the ionisation rate ζ per hydrogen particle. The dependence of this rate ζ on depth σ from the surface (expressed as g/cm^2) can be approximated by (see their Fig. 6)

$$\zeta(\sigma) = \frac{4 \cdot 10^{-18}}{e^{\sigma/115} + 1} \; [s^{-1}] \,. \tag{26}$$

This approximation for ζ is roughly constant up to a depth of ≈ 50 g/cm^2 and then starts to fall off exponentially with a length scale of 115 g/cm^2. It does not reproduce the slight initial increase of ζ between $\sigma = 0$ and $\sigma = 40$ g/cm^2 and the slightly steeper decrease of ζ for $\sigma \gg 500$ g/cm^2 of the ionisation rate obtained by Umebayashi and Nakano (1981) but the approximation (26) should be of sufficient accuracy for the cold part of the protostellar disk where the surface density is much less than 1 000g/cm^2.

The rate (26) is somewhat less than the standard rate of ionisation by cosmic rays used in cosmic chemistry, which generally assumes a rate coefficient $\zeta \approx 10^{-17}\,s^{-1}$ (e.g Lepp (1992) or Cecchi-Pestellini and Aiello (1992)). The large uncertainty in this rate is due to the poor knowledge of the low energy part of the cosmic ray energy spectrum and the way how different authors extrapolate to the low energy regime. Since the higher value of ζ used in astro-chemistry seems to reproduce better observed molecular abundances than the rather low value of $\zeta(\sigma = 0)$ according to (26), we changed for our model calculation the constant $4 \cdot 10^{-18}$ in Eq. (26) into $2 \cdot 10^{-17}$, i.e., we changed the value of $\zeta(0)$ to be in better accord with standard values, but we retain the dependence of ζ on σ as derived by Umebayashi and Nakano (1981).

Fig. 1 shows the ionisation rate $\zeta(s)$ for our disk model in the midplane of the accretion disk where the depth σ in Eq. (26) equals the surface density $\Sigma(s)$ given by Eq. (1). The surface density Σ in the region of the terrestrial planets is of the order of several 10^3 g·cm^{-2}. Thus, in the inner part of the protoplanetary disk the cosmic rays cannot penetrate deeply into the disk and the ionisation rate due to cosmic rays near the midplane of the disk is very small. The ion-molecule chemistry driven by cosmic ray ionisation in this part of the proto-planetary disk affects a thin surface layer only and it seems unlikely that this in turn has important consequences for the chemistry in the midplane of the disk. In the midplane of the accretion disk ionisation then is due to radioactive nuclei and thermal ionisation (cf. Fig. 1). From Eq. (1) we find that $\Sigma(s)$ drops to a value of ≈ 115 g·cm^{-2} at a distance of $s \approx 30$ AU. From this point on outwards the cosmic rays penetrate deep into the disk. Since in the region beyond the (present) position of Pluto the temperature in the disk is very low and all neutral-neutral reactions in this case are extremely slow, the chemistry in the outermost part of the protoplanetary accretion disk is strongly influenced by the cosmic-ray-driven ion molecule chemistry.

The possible shielding of cosmic rays by magnetic fields in the accretion disk is discussed by Dolginov and Stepinski (1994). This effect is not included in the determination of our ionisation rate since presently nothing is known about the order of magnitude of such effects. Also we have not yet included in our reaction network the cosmic-ray induced photoreactions by the mechanism described by Prasad and Tarafdar (1983).

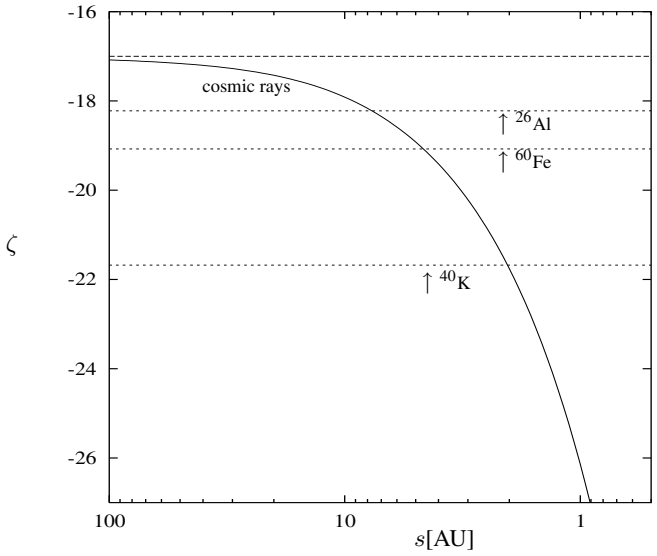

Fig. 1. Radial variation of the ionisation rate per hydrogen nucleus ζ in the central plane of the protoplanetary disk. The full line is the ionisation rate due to cosmic ray particles including the shielding by the overlying disk material. The dashed line is the unshielded rate. The dotted lines are the ionisation rates due to the decay of the two most important extinct radionuclides ^{26}Al and ^{60}Fe observed to have been present in the early solar system, and the most important longlived radioactive nucleus ^{40}K.

4.2. Ionisation by extinct radionuclides

A second important source of ionisation in the early solar system are the extinct radionuclides, i.e. unstable nuclides with halflifes of the order of 0.1 to 100 Myr which have all decayed since the formation of our planetary system 4.6 Gyr ago. Ionisation of the disk material by ^{26}Al has first been discussed by Consolmagno and Jokipii (1976). Ionisation by radioactive nuclei is also discussed by Umebayashi and Nakano (1981). For the case of circumstellar dust shells, ionisation by longlived radioactive nuclei has briefly been discussed by Glassgold (1995). We reconsider the process since some aspects of the problem are different in our case and since some data have been revised, especially the halflife of ^{60}Fe (Kutschera et al. 1984).

The possible candidates for extinct radionuclides and their decay modes are listed in Table 3. From studies of the isotopic composition of pristine material from the early days of our solar system found in certain meteorites it is known that at least some of these nuclei have been present at that time in the solar system (cf. Wasserburg and Papanastassiou 1982, Wasserburg 1985, Swindle 1993). The certain and likely identifications are shown in Table 3. It is believed that the observed short lived nuclei are not formed within the protoplanetary system (though this cannot be ruled out with complete certainty) but result from one or a few late nucleosynthetic events in dying stars just prior to the onset of collapse of the molecular cloud material into the

Table 3. Longlived radionuclides up to Bi with half-lifes between 10^5 and 10^8yr, their abundance ϵ and their decay modes to stable nuclei.

Nucleus	half-life yr	ϵ	decay-mode	freq.	energy MeV	β-energy MeV	γ-energy MeV	abundance
^{41}Ca	$1.02 \cdot 10^5$	6.34	$^{41}\mathrm{Ca} + e \rightarrow {}^{41}\mathrm{K} + \bar{\nu}$	100%	0.4214			$1.5\,10^{-8}$ ^{41}Ca/^{40}Ca
^{99}Tc	$2.13 \cdot 10^5$	—	$^{99}\mathrm{Tc} \rightarrow {}^{99}\mathrm{Ru} + \beta^- + \bar{\nu}$	100%	0.294	0.293		
^{36}Cl	$3.01 \cdot 10^5$	5.27	$^{36}\mathrm{Cl} \rightarrow {}^{36}\mathrm{Ar} + \beta^- + \bar{\nu}$	98%	0.7086	0.7093		
			$^{36}\mathrm{Cl} \rightarrow {}^{36}\mathrm{S} + \beta^+ + \nu$	2%	1.1421	0.115	ann.rad.	
			$^{36}\mathrm{Cl} + e \rightarrow {}^{36}\mathrm{S} + \nu$	0.002	1.1421			
^{208}Bi	$3.68 \cdot 10^5$	0.713	$^{208}\mathrm{Bi} + e \rightarrow {}^{208}\mathrm{Pb} + \bar{\nu}$	100%	2.880		2.61435	
^{26}Al	$7.1 \cdot 10^5$	6.39	$^{26}\mathrm{Al} \rightarrow {}^{26}\mathrm{Mg}^* + \beta^+ + \nu$	82%	4.0042	1.16	ann.rad.	$5\,10^{-5}$ ^{26}Al/^{27}Al
			$^{26}\mathrm{Al} + e \rightarrow {}^{26}\mathrm{Mg}^* + \bar{\nu}$	18%	4.0044		+ 1.80865 (99.8%)	
^{60}Fe	$1.5 \cdot 10^6$	7.60	$^{60}\mathrm{Fe} \rightarrow {}^{60}\mathrm{Co} + \beta^- + \nu$	100%	0.237	0.184	0.0586 (IT, 100%)	$1.6\,10^{-6}$ ^{60}Fe/^{56}Fe
	5.271		$^{60}\mathrm{Co} \rightarrow {}^{60}\mathrm{Ni} + \beta^- + \nu$	100%	2.824	0.315	1.17321+1.33247	
^{93}Zr	$1.5 \cdot 10^6$	2.61	$^{93}\mathrm{Zr} \rightarrow {}^{93}\mathrm{Nb} + \beta^- + \bar{\nu}$	100%	0.091		0.0304	
^{10}Be	$1.52 \cdot 10^6$	1.42	$^{10}\mathrm{Be} \rightarrow {}^{10}\mathrm{B} + \beta + \hat{\nu}$	100%	0.5559	0.555		
^{150}Gd	$1.8 \cdot 10^6$	1.07	$^{150}\mathrm{Gd} \rightarrow {}^{146}\mathrm{Sm} + \alpha$	100%	2.80	2.73		
^{81}Kr	$2.1 \cdot 10^5$	3.21	$^{81}\mathrm{Kr} + e \rightarrow {}^{81}\mathrm{Br} + \bar{\nu}$	100%	0.2807			
^{135}Cs	$2.3 \cdot 10^6$	1.12	$^{135}\mathrm{Cs} \rightarrow {}^{135}\mathrm{Ba} + \beta^- + \bar{\nu}$	100%	0.269	0.205		$\approx 1\,10^{-5}$ ^{135}Cs/^{133}Cs
^{97}Tc	$2.6 \cdot 10^6$	—	$^{97}\mathrm{Tc} + e \rightarrow {}^{97}\mathrm{Mo} + \bar{\nu}$	100%	0.320			
^{154}Dy	$3 \cdot 10^6$	1.15	$^{154}\mathrm{Dy} \rightarrow {}^{150}\mathrm{Gd} + \alpha$	100%	2.95	2.87		
^{53}Mn	$3.7 \cdot 10^6$	5.53	$^{53}\mathrm{Mn} + e \rightarrow {}^{53}\mathrm{Cr} + \bar{\nu}$	100%	0.5970			$6\,10^{-6}$ ^{53}Mn/^{55}Mn
^{98}Tc	$4.2 \cdot 10^6$	—	$^{98}\mathrm{Tc} \rightarrow {}^{98}\mathrm{Ru} + \beta^- + \bar{\nu}$	100%	1.80	0.40	0.65241+0.74535	
^{107}Pd	$6.5 \cdot 10^6$	1.70	$^{107}\mathrm{Pd} \rightarrow {}^{107}\mathrm{Ag} + \beta^- + \bar{\nu}$	100%	0.033	0.033		$9\,10^{-5}$ ^{107}Pd/^{110}Pd
^{182}Hf	$9. \cdot 10^6$	0.742	$^{182}\mathrm{Hf} \rightarrow {}^{182}\mathrm{Ta} + \beta^- + \bar{\nu}$	100%	0.37		0.2704	detected
	114.43 d		$^{182}\mathrm{Ta} \rightarrow {}^{182}\mathrm{W} + \beta^- + \bar{\nu}$	100%	1.814	0.25 (30%)	0.06775+0.1001	
						0.44 (20%)	+1.12127+1.22138	
						0.52 (40%)		
^{205}Pb	$1.51 \cdot 10^7$	1.97	$^{205}\mathrm{Pb} + e \rightarrow {}^{205}\mathrm{Tl} + \bar{\nu}$	100%	0.0512			detected
^{129}I	$1.7 \cdot 10^7$	1.51	$^{129}\mathrm{I} \rightarrow {}^{129}\mathrm{Xe} + \beta^- + \bar{\nu}$	100%	0.194	0.15	0.0396	$1.5\,10^{-4}$ ^{129}I/^{127}I
^{92}Nb	$3.7 \cdot 10^7$	1.40	$^{92}\mathrm{Nb} + e \rightarrow {}^{92}\mathrm{Zr} + \bar{\nu}$	100%	2.006		0.5611+0.9345	$1.5\,10^{-5}$ ^{92}Nb/^{93}Nb
^{146}Sm	$1.03 \cdot 10^8$	0.966	$^{146}\mathrm{Sm} \rightarrow {}^{142}\mathrm{Nd} + \alpha$	100%	2.50			$8\,10^{-3}$ ^{146}Sm/^{144}Sm

Data from the CRC Handbook (Lide 1995), element abundances from Anders and Grevesse (1989), abundances in the early solar system as collected by Cameron (1993) and Harper (1996).

protosun and the protoplanetary disk (e.g. Wasserburg 1985, Cameron 1993).

Most efficient for the ionisation of the disk material obviously are such nuclei which have (i) a high abundance, (ii) a high decay rate, but a halflife not smaller than $\approx 10^5$ yr in order that the nuclei still exist at the time when the accretion disk enters the viscous stage, (iii) a high decay energy, and (iv) which liberate most of their decay energy as charged particles or γ-rays which then in a subsequent series of events ionise the disk material. Nuclei which decay by electron capture often transfer most of their decay energy to the neutrino which is lost from the disk; the decay of such nuclei cannot contribute significantly to the ionisation of matter. Here we are interested in the earliest phase of the formation of our planetary system prior to the formation of the planets and the dissipation of the gaseous disk component. This so called viscous phase lasts for at most 10^6 years (Cameron 1988). An inspection of Table 3 shows the most likely candidates for ionisation by radioactive decay in this phase of the planetary system to be the nuclei ^{35}Cl, ^{26}Al and ^{60}Fe. All other possible candidates either have low decay energy, low general abundance of the parent and daughter elements which is incompatible with a high abundance of that isotope, or they decay by electron capture like the rather abundant ^{53}Mn and, thus, do not produce significant amounts of ionising radiation. For the problem of heating of planetesimals the same set of three nuclei has been proposed as possible heat sources for these bodies (Fish et al. 1960). Only if the bulk of these short lived nuclei have decayed then other more slowly decaying and less abundant nuclei may become important sources for the ionisation of matter.

From these three possible candidates only the existence of ^{26}Al and ^{60}Fe has definitely be confirmed for the early protoplanetary system. As for ^{35}Cl, nothing seems to be known about its presence or nonexistence in the early solar system. Because of the generally much lower abundance of the element Cl compared to the elements Al and Fe and because of its shorter halflife the ^{36} Cl cannot be as important for the ionisation of the disk material in the viscous phase of the accretion disk as is Al and Fe and we do not further consider this possible source of ionisation.

4.2.1. Decay of ^{26}Al

Lee et al. (1977) found an excess of the decay product ^{26}Mg of the ^{26}Al isotope in Ca-Al-rich inclusion of the Allende meteorite. Hence, at the time where these chondrules were formed, life ^{26}Al was present. Subsequently, the former existence of ^{26}Al has been confirmed by a ^{26}Mg excess in several other meteorites. Its abundance relative to the stable ^{27}Al isotope at the time of chondrule formation invariably has been found to be $5 \cdot 10^{-5}$ (Wasserburg and Papanastassiou 1982).

^{26}Al decays into the stable ^{26}Mg isotope via two possible routes:

1. by a β^+ decay $^{26}\mathrm{Al} \rightarrow {}^{26}\mathrm{Mg}^* + \beta^+ + \nu$ with a maximum energy of the positron of 1.16 MeV and with a frequency of 82% and
2. by electron capture $^{26}\mathrm{Al} + \mathrm{e} \rightarrow {}^{26}\mathrm{Mg}^* + \bar{\nu}$ with a frequency of 18%.

In both cases an excited ^{26}Mg nucleus is formed by the transition which is de-excited by a radiative transition resulting in the emission of a photon with an energy of either 1.809 MeV with a frequency of 99.8% or of 1.130 MeV energy with a frequency of 0.2% (we do not consider this rare decay mode in the following). The line at 1.809 MeV was predicted to be visible as a sharp interstellar γ line emitted by material ejected in a supernova explosion (Ramaty and Lingenfelter 1977) and, indeed, this line has been observed (Mahoney et al. 1984). It is now a well known source of galactic γ line radiation. The main source of galactic ^{26}Al γ-rays are likely to be ejecta of young stellar objects like Wolf-Rayet stars and core collapse supernovae (eg. del Rio et al. 1996). ^{26}Al also is likely to be produced as a by-product of H-shell burning in AGB-stars and it may be that all of the ^{26}Al observed to be present at the instant of solar system formation results from the contamination of the molecular cloud material with the ejecta from one single AGB-star (Wasserburg et al. 1994). A supernova origin of most of the extinct radionuclides cannot be excluded, however (Harper 1996).

The average energy of the β^+ resulting from the decay of ^{26}Al is $\bar{E}_\beta = 0.66$ MeV. These positrons collisionally excite and ionise the particles of the disk material and loose by these processes their energy. The remaining fraction of energy of 0.5 MeV is carried away by the neutrino which leaves the accretion disk without further interaction.

β particle ranges for particles of $\approx .5$ MeV energy are of the order of $0.2\,\mathrm{cm}^2/\mathrm{g}$. These particles are stopped completely within the disk. Since aluminium is completely bound in dust grains the decaying ^{26}Al nuclei are located within such dust particles and since interstellar dust grains are sub-micron sized, the β^+ particles are not stopped within their parent dust grains but somewhere in the disk. If the β^+ come near to rest, they annihilate and form a pair of γ's with 0.511 MeV each.

Thus, each β^+ decay of ^{26}Al injects one 1.809 MeV and two 0.511 MeV γ's into the disk. γ's with an energy of the order of 1 MeV loose their energy predominantly by Compton scattering which transmits part of the γ-energy to the recoil electron. The scattering cross section for the 1.809 MeV quanta according to the Klein-Nishina formula (Clayton 1968) is $\sigma = 1.55\,10^{-25}\,\mathrm{cm}^2$ and for the .511 MeV quanta is $\sigma = 2.86 \cdot 10^{-25}\,\mathrm{cm}^2$. The mean range of these photons in the disk material is

$$R = \frac{\rho}{n_e \sigma} = \frac{m_\mathrm{H}}{\sigma} \, \frac{1 + 4\epsilon_\mathrm{He}}{1 + 2\epsilon_\mathrm{He}} \, . \tag{27}$$

Here we approximated the mean density of electrons, irrespective whether they are bound or free, by

$$n_\mathrm{e} = \frac{\rho}{m_\mathrm{H}} \, \frac{1 + 2\epsilon_\mathrm{He}}{1 + 4\epsilon_\mathrm{He}} \tag{28}$$

We obtain $R = 1.26 \cdot 10^1\,\mathrm{g/cm}^2$ and $R = 6.80 \cdot 10^0\,\mathrm{g/cm}^2$ for the 1.809 MeV and 0.511 MeV γ's, respectively.

In Appendix A it is shown that after roughly $N = 10$ scattering events these γ-quantums have transferred their energy nearly completely to energetic recoil electrons. Since scattering of high energy γ quantums is strongly peaked in the forward direction the γ's move on the average $\approx N$ times of the above mean free path length away from the point of their creation until they have lost their energy and eventually become photoabsorbed or perhaps some fraction of the strongly degraded γ's diffuses out of the disk. Compared with a surface density of the protoplanetary accretion disk of several $10^3\,\mathrm{g/cm}^2$ at the position of the inner planets this means that the γ's transfer all of their energy within the disk to energetic recoil electrons. These then ionise the matter by collisional ionisation while they are slowed down.

If the surface density Σ of the accretion disk drops below $\approx 150\,\mathrm{g/cm}^2$, part of the γ's can diffuse out of the disk before loosing all of their energy. This would reduce the ionisation rate. For the stationary disk model of Sect. 2 this requires a radius $s \gtrsim 100$ AU, but at such large distances our stationary disk model is not likely to be applicable and our calculation is restricted to smaller distances. Calculating the ionisation by extinct radionuclides in the outer parts of the accretion disk will be a much more difficult task since one has to solve the radiative transfer problem for the γ quantums across the disk in that part of the accretion disk.

In the decay mode of ^{26}Al by electron capture the energy of decay to the excited states of ^{26}Mg is carried away by the neutrino. The transition leaves an excited atom which is de-excited by Auger electrons, but these have much smaller energies than the β^+ particles and yield only a negligible contribution to the

Table 4. Ionisation rates by extinct radionuclides in the early solar system

Isotope	^{26}Al	^{60}Fe	^{135}Cs	^{107}Pd	^{129}I
ζ[s^{-1}]	$6.0\,10^{-19}$	$8.4\,10^{-20}$	$5\,10^{-27}$	$1\,10^{-27}$	$3\,10^{-26}$
Isotope	^{92}Nb	^{146}Sm	^{244}Pu		
ζ[s^{-1}]	$1\,10^{-26}$	$5\,10^{-26}$	$2\,10^{-27}$		

ionisation of matter. The subsequent γ decay of the ^{26}Mg nucleus, however, contributes to the ionisation of the matter by the emission of the 1.809 MeV γ quantum.

The ionisation rate due to the decay of ^{26}Al therefore is determined by the collisional ionisation of matter by the fast β^+ particles and the fast recoil electrons from Compton scattering of the γ's. Assuming $W = 36$ eV as the average energy required to create an ion pair in the H-He mixture as Umebayashi and Nakano (1981) did (cf. also Dalgarno and Griffing 1958), an abundance of Al of $3.04 \cdot 10^{-6}$ (Anders and Grevesse 1989), a relative abundance of ^{26}Al to ^{27}Al of $5 \cdot 10^{-5}$ at the time of formation of the Ca-Al-rich inclusions, and a halflife of $\tau = 7.1 \cdot 10^5$ yr, we obtain an ionisation rate of the disk material by ^{26}Al decay of

$$\zeta = \epsilon \cdot \frac{0.82 \cdot (\bar{E}_\beta + 2 \cdot m_e c^2 + E_\gamma) + 0.18 \cdot E_\gamma}{W\tau} = 6.0 \cdot 10^{-19}\ \mathrm{s}^{-1} \quad (29)$$

per hydrogen nucleus.

4.2.2. Decay of ^{60}Fe

The iron isotope ^{60}Fe has been present in the early solar system according to the study of Birk and Lugmayr (1988) of Ni isotopes in Allende inclusions which clearly revealed an excess of the decay product ^{60}Ni of the ^{60}Fe isotope. Its abundance at the time of condensation of the material contained in Allende was derived as $1.6 \cdot 10^{-6}$ for ^{60}Fe/^{56}Fe. This fits to similar findings of ^{60}Fe in differentiated meteorites (Shukolyukov and Lugmair 1993) which solidified several Myr's later. The derived abundance of 10^{-8} for ^{60}Fe/^{56}Fe at that instant fits nicely to an abundance of $1.6 \cdot 10^{-6}$ at the instant when the Ca-Al-rich inclusions were formed. Cameron (1993) points to the fact that this isotope of Fe is produced simultaneously with ^{107}Pd, ^{135}Cs, and ^{182}Hf in s-process nucleosynthesis in the same AGB star which is thought to be responsible for the formation of the definitely observed nuclei ^{107}Pd and ^{135}Cs. The observed abundance of ^{60}Fe fits rather well to the abundance expected for ^{60}Fe if it is co-produced with ^{107}Pd.

^{60}Fe decays into ^{60}Co by β decay with a maximum β energy of 0.184 MeV with a halflife of $1.5 \cdot 10^6$yr, followed by an isomeric transition with a halflife of 10.47 min to the ground state of ^{60}Co with the emission of a 0.059 MeV γ-quantum. The ^{60}Co decays into an excited state of ^{60}Ni by a beta decay with a maximum β energy of 0.315 MeV and a halflife of 5.26 yr. This is immediately followed by two radiative transitions to the ground state of ^{60}Ni with emission of two γ's with 1.173 MeV and 1.332 MeV each. Only a tiny fraction of the β decays of ^{60}Co goes to the excited state of ^{60}Ni 1.332 MeV above the ground state followed by the emission of the 1.332 MeV γ-quantum only. We neglect this rare decay mode.

Table 5. Ionisation rates by longlived radionuclides in the early solar system 4.6 Gyr's ago. ϵ is the abundance of the isotope in the early solar system and ζ is the ionisation rate per H nucleus

isotope	decay mode	halflife [yr]	energy [MeV]	ϵ	rate ζ s^{-1}
^{40}K	β (89.3%)	$1.3\,10^9$	0.54	$5.9\,10^{-10}$	$2.1\,10^{-22}$
	e-capt.	$1.2\,10^{10}$	1.5		
^{87}Rb	β	$4.9\,10^{10}$	0.097	$7.8\,10^{-11}$	$1.4\,10^{-25}$
^{147}Sm	α	$1.1\,10^{11}$	2.2	$1.4\,10^{-12}$	$2.6\,10^{-26}$
^{232}Th	α	$1.4\,10^{10}$	4.0	$2.6\,10^{-12}$	$6.7\,10^{-25}$
^{235}U	α	$7.0\,10^8$	4.6	$1.5\,10^{-12}$	$8.6\,10^{-24}$
^{238}U	α	$4.5\,10^9$	4.2	$8.9\,10^{-13}$	$7.4\,10^{-25}$

With respect to range of the γ's in the accretion disk the considerations for the case of ^{26}Al are valid for the present case, too.

The ionisation rate due to the decay of ^{60}Fe therefore is determined by the collisional ionisation of matter by the fast electrons from the β decays of ^{60}Fe and ^{60}Co and the fast recoil electrons from Compton scattering of the γ's from the radiative transitions in ^{60}Co and ^{60}Ni. The halflife of ^{60}Co is so much smaller than the halflife of ^{60}Fe that the decay of ^{60}Co to ^{60}Ni can be considered as instantaneously following the ^{60}Fe decay. Using $W = 36$ eV as the average energy required to create an ion pair in the H-He mixture (Umebayashi and Nakano 1981), an abundance of Fe of $3.24 \cdot 10^{-5}$ (Anders and Grevesse 1989), a relative abundance of ^{60}Fe to ^{56}Fe of $1.6 \cdot 10^{-6}$ at the time of formation of the Ca-Al-rich inclusions, and a halflife of $\tau = 1.5 \cdot 10^6$ yr, we obtain an ionisation rate of the disk material by ^{60}Fe–decay of

$$\zeta = \epsilon \cdot \frac{\bar{E}_\beta + E_\gamma}{W\tau} = 8.4 \cdot 10^{-20}\ \mathrm{s}^{-1} \quad (30)$$

per hydrogen nucleus.

4.2.3. Ionisation by other extinct radionuclides

Other extinct radionuclides than ^{26}Al and ^{60}Fe are not important for the ionisation of the primordial solar nebula. We estimate the rates for the isotopes with known abundance in the early solar system as above and obtain the results shown in Table 4. Their ionisation rate can be neglected compared to that of ^{26}Al and ^{60}Fe and even if these two shortlived nuclei have decayed, the ionisation by the longlived nuclei is more important than that of the less abundant extinct radionuclei listed in Table 4.

4.2.4. Ionisation by longlived radionuclides

For the longlived radionuclides we calculate the ionisation rate as above using again a value of $W = 36\,\mathrm{eV}$ for the average energy loss of α particles per created ion pair (Umebayashi and Nakano (1981). Isotope abundances and data for the decays are taken from Lide (1995), present element abundances from Anders and Grevesse (1989). We calculated the abundance of the radioactive isotopes in the early solar system by assuming that the Ca-Al-rich inclusions formed 4.5578 Gyr ago (Lugmair and Galer 1992). The resulting ionisation rates per H nucleus are shown in Table 5. The results are not very different from the results of Umebayashi and Nakano (1981). By far the most important longlived nucleus for ionisation in the early solar system was ^{40}K. At the time when the Ca-Al-rich inclusions formed, the ionisation rate by this nucleus, however, is negligible compared to the ionisation rate due to extinct radionuclides (cf. Fig. 1). It becomes only important if the ionisation rate by ^{60}Fe drops below that of ^{40}K which happens to occur $\approx 9\,$Myr's after the formation of the Ca-Al-rich inclusions. At that time there exist already asteroidal sized bodies in the solar system (Weidenschilling and Cuzzi 1993) and the gaseous disk is likely to be (at least partly) dispersed (Beckwith and Sargent 1993). Thus, longlived radioactive nuclei are not an important source of ionisation in the early protoplanetary system.

4.3. Ionisation by UV photons

We consider in this work the possibility of ionising the atoms and molecules by UV photons. Because the disk is optically thick both in the radial and vertical direction, we will exclude the possibility of ionisation by direct irradiation with UV photons from the central star. External UV sources or scattered light from the central star could provide an influx of UV photons in the vertical direction. However, we have no information about the magnitude of the UV flux from such sources and a crude estimate made in Paper II has shown that only the thin outer layers could be affected by such photoprocesses while our calculation refers mainly to the midplane of the disk.

We assume in the following that the UV radiation present in the midplane of the disk equals the thermal black body radiation field with a temperature equal to the temperature in the midplane of the disk. This is justified since the disk is optically thick in the UV in the vertical direction. We include in our reaction network ionisation and recombination processes between ions and electrons

$$\mathrm{X} + h\nu \longleftrightarrow \mathrm{X}^+ + \mathrm{e}^- \,. \tag{31}$$

Such processes are mainly important at temperatures in the disk where most of the molecules are already dissociated. We restrict, for this reason, in the present calculation the consideration of photoionisation to atoms and ions.

The photoionisation rate for some species X is given by

$$R_{\mathrm{ion}} = n_{\mathrm{X}} \int_{\nu_0}^{\infty} \frac{4\pi J_\nu}{h\nu}\,\sigma_\nu d\nu \equiv k(T)\,n_{\mathrm{X}}\,. \tag{32}$$

n_{X} is the particle density, J_ν is the average radiation intensity, σ_ν is the photoionisation cross section and $h\nu_0$ is the ionisation energy. The rate of the reverse process (recombination) is given in terms of a recombination coefficient $\alpha(T)$. The recombination rate is

$$R_{\mathrm{rec}} = \alpha(T)\,n_{\mathrm{X}^+} n_{\mathrm{e}^-} \tag{33}$$

In the particular case of thermal equilibrium between neutral atoms, ions and photons we have

$$n_{\mathrm{X}} \int_{\nu_0}^{\infty} \frac{4\pi B_\nu}{h\nu}\sigma_\nu d\nu = \alpha(T)\,n_{\mathrm{X}^+} n_{\mathrm{e}^-}\,, \tag{34}$$

i.e.

$$\frac{n_{\mathrm{X}^+} n_{\mathrm{e}^-}}{n_{\mathrm{X}}} = \frac{k(T)}{\alpha(T)} = S(T)\,. \tag{35}$$

This is the well known Saha equation, i.e. the law of mass action applied to the special type of reaction (31). If we know the recombination coefficients $\alpha(T)$ we are able to calculate the photoionisation rates $k(T)$ in a thermodynamic equilibrium state or vice versa. The relation $k(T) = \alpha(T)S(T)$ (Milne relation) is valid even if the species X, X^+ and the electrons are not in chemical equilibrium, as long as the local radiation field is the black body radiation field, the velocity distribution of the electrons is the Maxwellian velocity distribution and if excited states of the particles are thermally populated. We assume that these basic assumptions of LTE are valid in the midplane of the disk.

The rate of change of the particle density of species X then is given by

$$\frac{dn_{\mathrm{X}}}{dt} = \alpha(T)\,(n_{\mathrm{X}^+} n_{\mathrm{e}^-} - S(T) n_{\mathrm{X}}) \tag{36}$$

and we have of course

$$\frac{dn_{\mathrm{X}^+}}{dt} = -\frac{dn_{\mathrm{X}}}{dt}\,. \tag{37}$$

We consider the ionisation of all the abundant elements H, C, N, O, Mg, Si, S, and Fe which are included in our calculation of the chemistry, and additionally we consider the readily ionised atoms Al, Ca, Na, and K which serve as electron donators. Only the first ionisation stage of all these atoms is included in the calculation since we do not extend the integration into the hot boundary layer near the star. The recombination coefficients $\alpha(T)$ for the elements are taken from Landini and Monsignori Fossi (1990).

Besides ionisation of the neutral atoms we consider the formation of H^- according to the reaction

$$\mathrm{H} + \mathrm{e}^- \longleftrightarrow \mathrm{H}^- + h\nu\,. \tag{38}$$

H^-, though never being very abundant, is a very important species because it is responsible for the so called *viscous instability* (see Paper II) which occurs in the innermost parts of the disk.

We expect that the thermal ionisation according to (31) in the warmest region of the accretion disk provides large amounts of ions and free electrons while the reverse process of recombination consumes most of the free electrons provided by cosmic rays and nuclear decay induced ionisation in the cold part of the disk. Test calculations have shown that especially the recombination reaction (38) to H^- is the most important process for electron consumption in the outer parts of the disk. These ionisation and recombination processes should substantially modify the whole chemistry in the accretion disk.

The dust forming elements Si, Fe, and Mg and the elements Na, Al, K, and Ca are not subject to ionisation until they are released into the gas phase during dust destruction. The modeling of their injection into the gas phase is explained in Sect. 3.3.

5. Initial conditions

We determine the chemistry in the accretion disk by solving the rate equations in a comoving frame which follows the motion of a gas parcel from the cold outer part of the accretion disk down to the hot temperature region close to the star. The initial conditions for the integration of the rate equations for the chemistry are the same as that adopted in Paper II except for the molecule H_2S, which is now assumed to be present in the gas phase at the outer edge of the disk. For the reasons given in Sect. 3.3, we consider that 50 % of the available S is locked in hydrogen sulfide. The remaining 50 % are supposed to be bound in troilite. We use in the present work the abundances given by Anders and Grevesse (1989) and Grevesse and Noels (1993) (cf. Table 2 in Paper II).

With $N_{\rm H} = 2n_{\rm H_2} + n_{\rm H}$ (total amount of hydrogen nuclei) and the abundance $\epsilon_{\rm X}$ for a species X, we prescribe the following initial concentrations:

$$n_{\rm H} = 10^{-5}\, N_{\rm H}\,, \tag{39}$$

$$n_{\rm N_2} = \frac{1}{2}\epsilon_{\rm N} N_{\rm H}\,, \tag{40}$$

$$n_{\rm He} = 0.1 N_{\rm H}\,, \tag{41}$$

$$n_{\rm CO} = 0.3\epsilon_{\rm C} N_{\rm H}\,, \tag{42}$$

$$n_{\rm H_2O} = (\epsilon_{\rm O} - 0.3\epsilon_{\rm C} - 4\epsilon_{\rm Si}) N_{\rm H}\,, \tag{43}$$

$$n_{\rm H_2S} = \frac{1}{2}\epsilon_{\rm S} N_{\rm H}\,. \tag{44}$$

$n_{\rm H_2}$ is determined from

$$\frac{P}{kT} = n_{\rm H_2} + n_{\rm H} + n_{\rm N_2} + n_{\rm He} + n_{\rm H_2S}\,. \tag{45}$$

The particle densities of all other species are initially put to zero.

This chemical composition is prescribed at the outer edge of the disk. We choose in this calculation an outer radius of 40 AU for the disk, which corresponds to the observed disks (Ruden and Pollack 1991) and to the size of our Solar System.

Our choice of the initial conditions does not consider that disk material at even large distances $s > 40$ AU from the protosun may have admixtures of material which originally landed in the hot central regions of the accretion disk during the infall phase. Part of this material drifts outwards while angular momentum is redistributed during the early disk evolution (up to distances as large as 100 AU) and later is intermingled with material landing at large distances from the star on the cold outer parts of the accretion disk, as has been pointed out by Cassen (1994). This means that during the viscous stage of the disk evolution the material drifting inwards from very cold outer regions of the protoplanetary accretion disk is likely to be contaminated by matter which was subject to strong chemical processing in hot regions of the disk during the early infall phase. How this changes the initial composition of the gas can only be determined by calculating the complete time evolution of a protoplanetary disk from the early infall up to the late viscous stage including the chemical processing of the material (gas+dust). Such models are presently not available.

6. Results

In this section we present our new results for the chemistry within the protoplanetary disk. We will discuss in detail the sulfur (Sect. 6.1) and the nitrogen (Sect. 6.2) chemistry, which both are strongly modified as compared to our previous results in Paper I and II by the ion-molecule reactions now included in our reaction network.

Figs. 2, 4 and 6 show the abundances of the neutral species from the outer edge (40 AU) of the disk down to a point close to the center (≈0.07 AU). Figs. 3, 5 and 7 show the abundances of the ions and of helium in the same region. A detailed description of the carbon and silicon chemistry can be found in Paper II. The addition of ionisation processes to the reaction network does not modify substantially the chemistry of these elements and our previous results are still valid.

6.1. The sulfur chemistry

This chemical system is strongly modified compared to the conclusions in our previous papers. The presence of hydrogen sulfide combined with the ionisation processes and the ion-molecule reactions now included in the reaction network induces an unexpected chemistry in the outer and middle parts of the protoplanetary disk (Fig.2 and 3). Our results for the chemical composition of the disk material at the actual location of the Earth are modified too.

The supposed presence of hydrogen sulfide in the outer parts of the protoplanetary disk has important consequences for the whole sulfur chemistry (Fig. 2). First of all we see that the presence of the hydrogen sulfide molecules at the outer disk edge (≈30 AU) immediately leads to the formation of large amounts of free sulfur atoms. The free S atom is formed as follows: In a first step a CO molecule in the gas phase is ionised by cosmic rays (ionisation by cosmic rays dominates over that by radionuclides in the outer part of the disk, cf. Fig. 1). The CO^+ then neutralises again in a charge transfer reaction with H_2S

$$\mathrm{CO^+ + H_2S \longrightarrow CO + H_2S^+}\,. \tag{46}$$

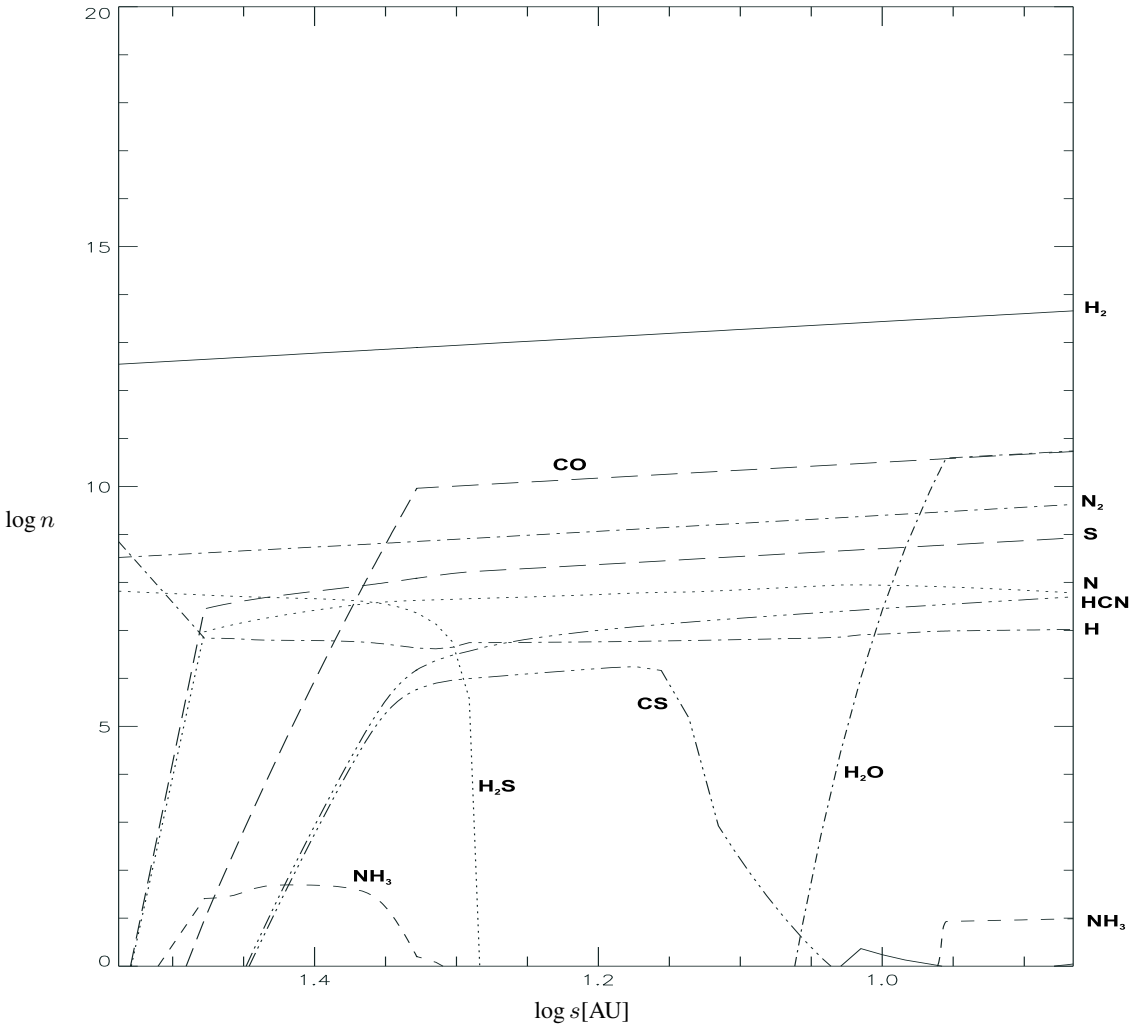

Fig. 2. Particle densities of neutral species in the external regions of the accretion disk.

The molecular ion H_2S^+ then is dissociated by recombination with a free electron to provide free sulfur and hydrogen atoms

$$H_2S^+ + e^- \longrightarrow S + 2H\,. \tag{47}$$

Because of the high efficiency of the reactions (46) and (47) it is questionable wether the existence of H_2S in the gas phase is possible in the presence of gas phase CO. Our calculation shows that hydrogen sulfide can exist only if most of the carbon monoxid is frozen onto the grains. If the CO is not frozen and if the ionisation processes are efficient enough, then H_2S should be destroyed very quickly. This conversion of H_2S into S only slowly proceeds for $s \gtrsim 23$ AU since most of the CO is frozen onto grains. At $s \approx 23$ AU the remaining fraction of the hydrogen sulfide then quickly disappears once the CO ice layers on the grains are vapourised.

The formation of substantial amounts of the ion S^+ is inhibited by its efficient recombination with free electrons. The few observed ions S^+ are the product of a charge transfer reaction between the free sulfur atoms produced in reaction (47) and H^+

$$S + H^+ \longrightarrow S^+ + H\,. \tag{48}$$

More generally, the H^- formation reaction (38) is very active at low temperatures and consumes nearly all free electrons. The very meager ion-molecule chemistry obtained in our protoplanetary disk model as compared to the rich ion-molecule chemistry obtained in model calculations for molecular clouds is the consequence of these two important electron consumption reaction.

According to our model calculation quite a high amount of CS is formed in the region between about 25 AU (≈22 K) and 12 AU (≈85 K). This molecule forms once CO is injected into the gas phase by vapourisation of the CO ice layers of the grains. As in the case of the hydrogen sulfide comsumption, the first step in the formation of CS is the ionisation of the carbon monoxid molecules by cosmic rays. The molecular ions CO^+ have a lower binding energy (8.34 eV) than CO and a dissociative recombination with free electrons can occur (such

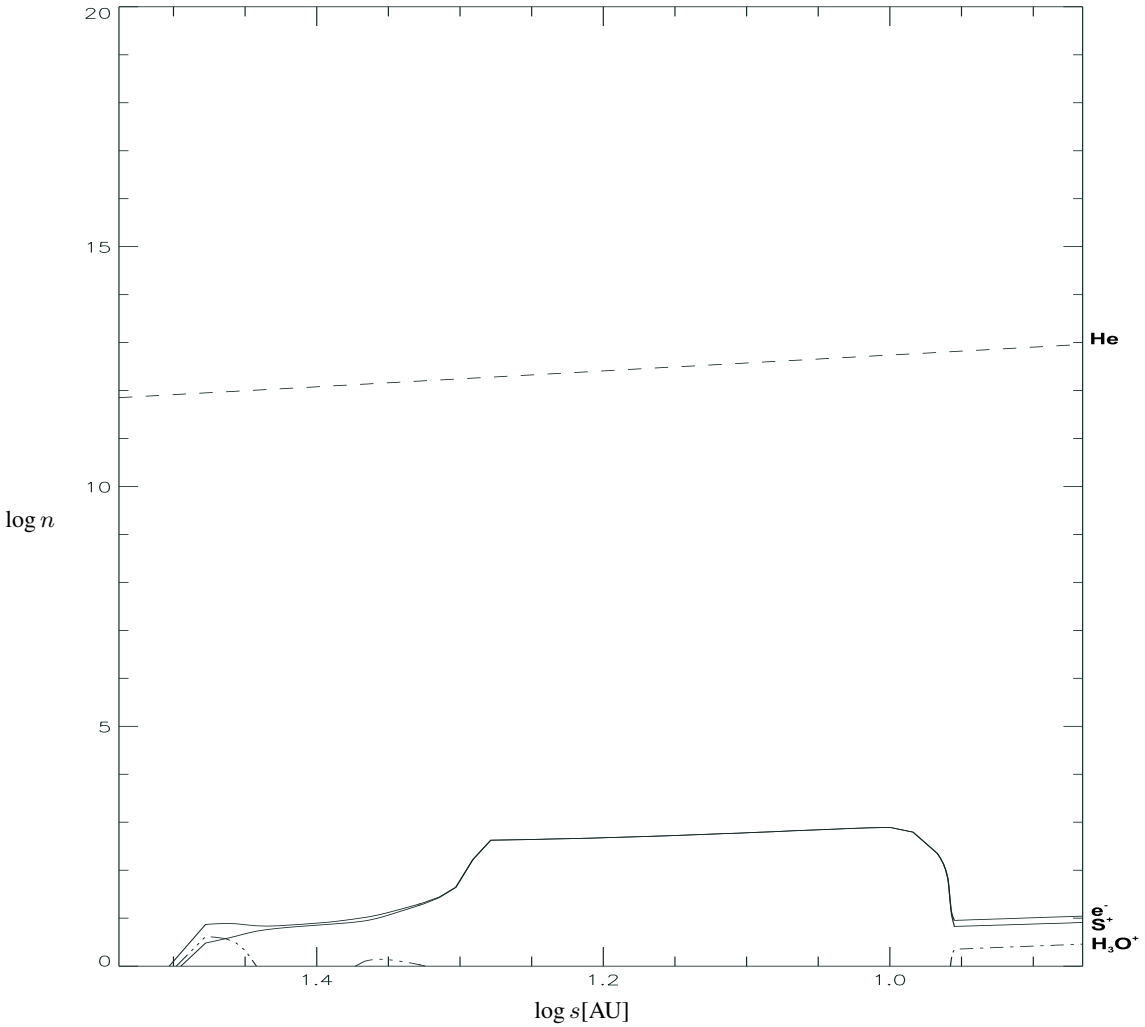

Fig. 3. Particle densities of ions in the external regions of the accretion disk.

dissociative recombinations are very active at low temperatures) leading to free carbon atoms

$$CO^+ + e^- \longrightarrow C + O\,. \tag{49}$$

These carbon atoms react very quickly with the molecular ion H_2S^+ formed in the pathway (46) to form the molecular ion HCS^+

$$H_2S^+ + C \longrightarrow HCS^+ + H\,. \tag{50}$$

A dissociative recombination then results in the formation of CS

$$HCS^+ + e^- \longrightarrow CS + H\,. \tag{51}$$

CS disappears at about 12 AU by a charge transfer reaction with H^+

$$CS + H^+ \longrightarrow CS^+ + H\,. \tag{52}$$

followed by a dissociative recombination

$$CS^+ + e^- \longrightarrow S + C\,. \tag{53}$$

The presence of considerable amounts of CS in the external parts of our disk's model is a very important result, since this molecule has been observed in protostellar sources (Ohashi et al. 1991), in the circumstellar disk HL Tauri (Blake et al. 1992) and more recently in the T Tauri stars DM Tau and GG Tau (Dutrey et al. 1996). In our previous work, CS formed as an *intermediate* product only in the region of the terrestrial planets. The ionisation processes now allow the formation of this molecule in observable quantities.

At about 2 AU ($T \approx$700 K) troilite begins to be decomposed. As we have seen in Paper II the injected sulfur atoms induce a very rich chemistry in the region of the terrestrial planets (between 2 and 0.8 AU). Fig. 8 shows the sulfur bearing species in this region. Due to the presence of free sulfur atoms for ($s \gtrsim 7.3$ AU) the sulfur chemistry shows some modifications as compared to our previous results (Fig. 6 in Paper II) where

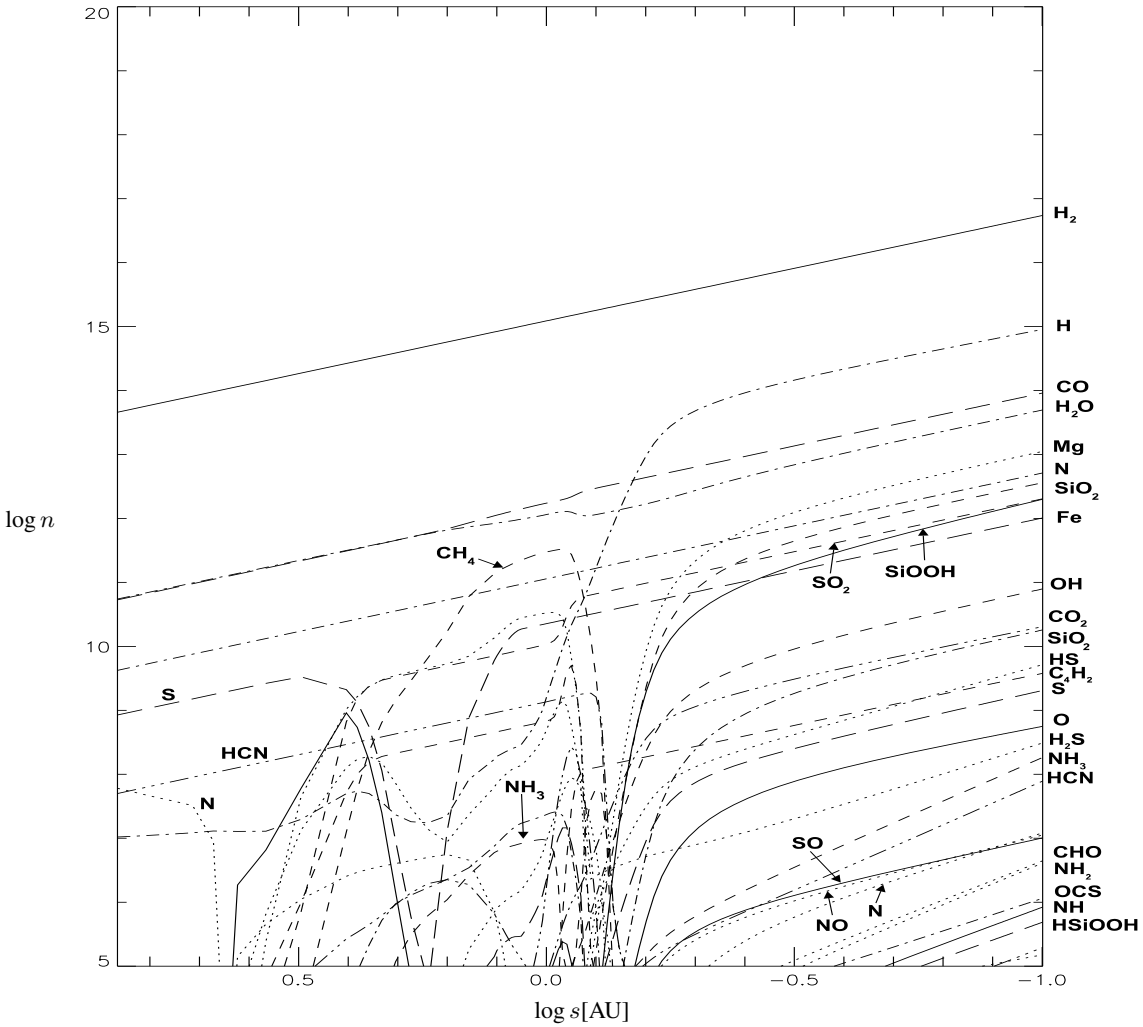

Fig. 4. Particle densities of neutral species in the regions of the accretion disk where the terrestrial planets are actually located.

only hydrogen sulfide molecules were present. However, the chemical pathways are essentially the same and we refer to Paper II for a detailed description.

Fig. 6 shows, as is to be expected, that all the neutral molecular species are destroyed in the innermost region of the disk because of the high temperature. Only free atoms, ions S^+, and some ions SO^+ are present in that region with significant abundance (Fig. 7). The key process leading to the formation of S^+ is photoionisation according to the process (31)

$$S + h\nu \longleftrightarrow S^+ + e^- \,. \tag{54}$$

The ions S^+ then reacts with OH to form the SO^+

$$S^+ + OH \longrightarrow SO^+ + H \,. \tag{55}$$

6.2. The nitrogen chemistry

The ionisation processes have dramatic and unexpected consequences for the chemistry of nitrogen bearing compounds. The most important molecule of this chemical system is N_2. It contains at the beginning all of the available N. Fig. 2 shows that at the outer edge of the disk free N atoms are formed very quickly. At a distance of 22 AU, about 3% of the available nitrogen is present as free atoms. Without the ionisation processes, as we have seen in our previous calculations, no process was able to break the extremely strong N_2 bond. The free nitrogen atoms now are available for chemical reactions which do not occur in the absence of ionisation processes.

The key reaction for the destruction of N_2 and therefore for the whole nitrogen chemistry is the same process that initiates the nitrogen chemistry in molecular clouds

$$N_2 + He^+ \longrightarrow N^+ + N + He \,. \tag{56}$$

He^+ forms as a product of the He ionisation by cosmic rays and the radio nuclides. N^+ can also be formed by ionisation of N by the cosmic rays (c.r.)

$$N + \text{c.r.} \longrightarrow N^+ + e^- \,. \tag{57}$$

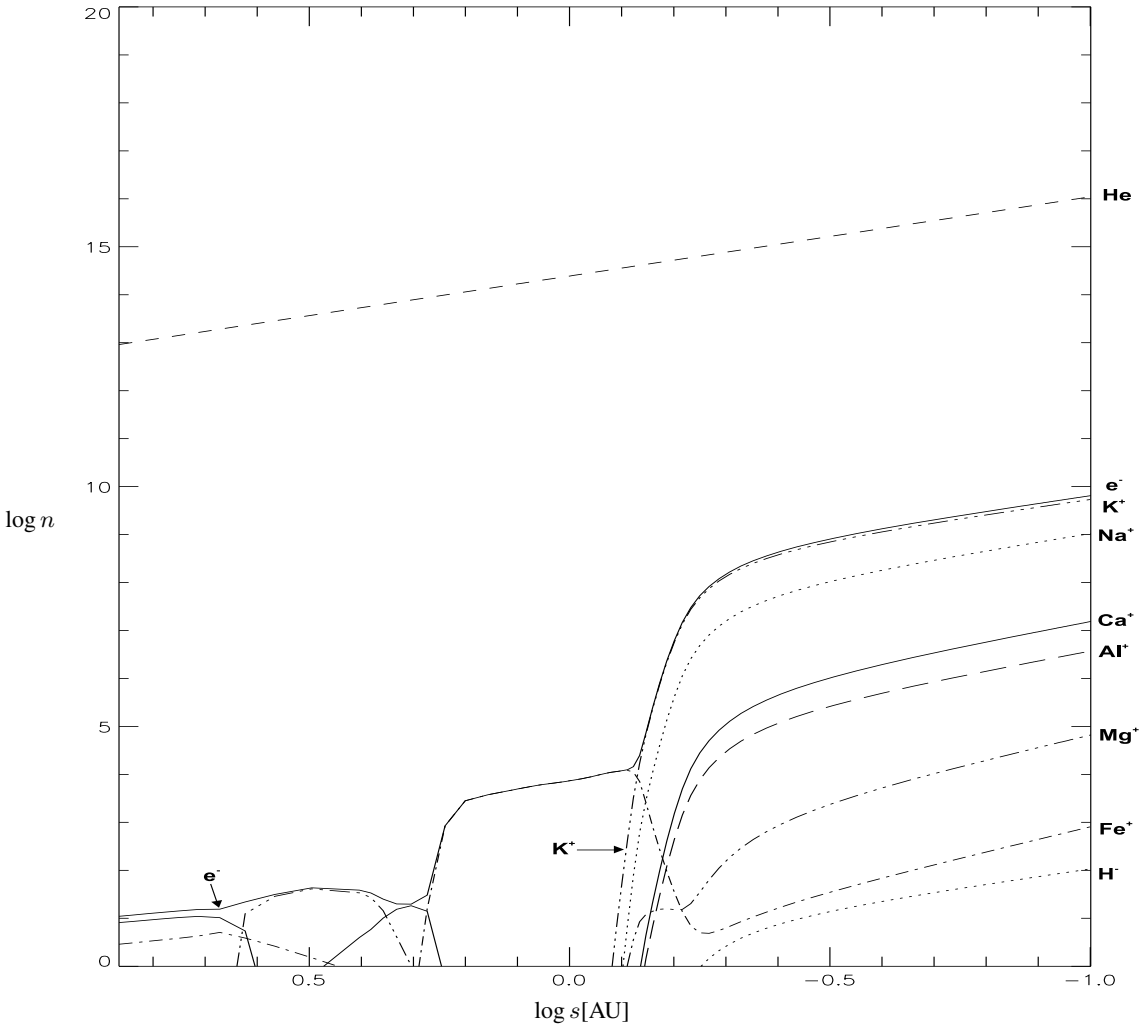

Fig. 5. Particle densities of ions in the regions of the accretion disk where the terrestrial planets are actually located.

but this process, because of the high helium density, is not as efficient as (56).

The next step following the formation of N^+ is the formation of NH_i^+ molecules in the following reaction chain

$$N^+ \overset{+H_2}{\longleftrightarrow} NH^+ \overset{+H_2}{\longleftrightarrow} NH_2^+ \overset{+H_2}{\longleftrightarrow} NH_3^+ \overset{+H_2}{\longleftrightarrow} NH_4^+ . \quad (58)$$

The different ions of this reaction chain can recombine with free electrons to form the neutral molecules NH, NH_2 and NH_3

$$NH_2^+ + e \longrightarrow N + H \quad (59)$$
$$\longrightarrow NH + H \quad (60)$$
$$NH_3^+ + e \longrightarrow NH_2 + H \quad (61)$$
$$\longrightarrow NH + H + H \quad (62)$$
$$NH_4^+ + e \longrightarrow NH_3 + H \quad (63)$$
$$\longrightarrow NH_2 + H + H . \quad (64)$$

This is the source of the NH_3 which is formed in considerable quantities in the region around $s \approx 1$ AU (cf. Fig. 4).

The NH_2 formed in the dissociative reaction can react with the ion C^+ and forms HCN^+ according to the rapid reaction

$$NH_2 + C^+ \longrightarrow HCN^+ + H . \quad (65)$$

A very efficient charge transfer reaction between HCN^+ and S then finally leads to formation of HCN

$$HCN^+ + S \longrightarrow HCN + S^+ . \quad (66)$$

These reactions are responsible for the formation of high amounts of cyanide inside a radius of $s \approx 25$ AU ($T \gtrsim 22$ K). It is interesting to point out, that the starter molecule NH_2 for cyanide formation can be formed by a completely neutral chemistry according to the reactions

$$N \overset{+H_2}{\longleftrightarrow} NH \overset{+H_2}{\longleftrightarrow} NH_2 \overset{+H_2}{\longleftrightarrow} NH_3 . \quad (67)$$

The first reaction of this chain, however, has a high activation energy barrier (10 700 K) and for this reason is kinetically forbidden in low temperature regions of the disk where HCN actually forms according to our model calculation. The ionisation

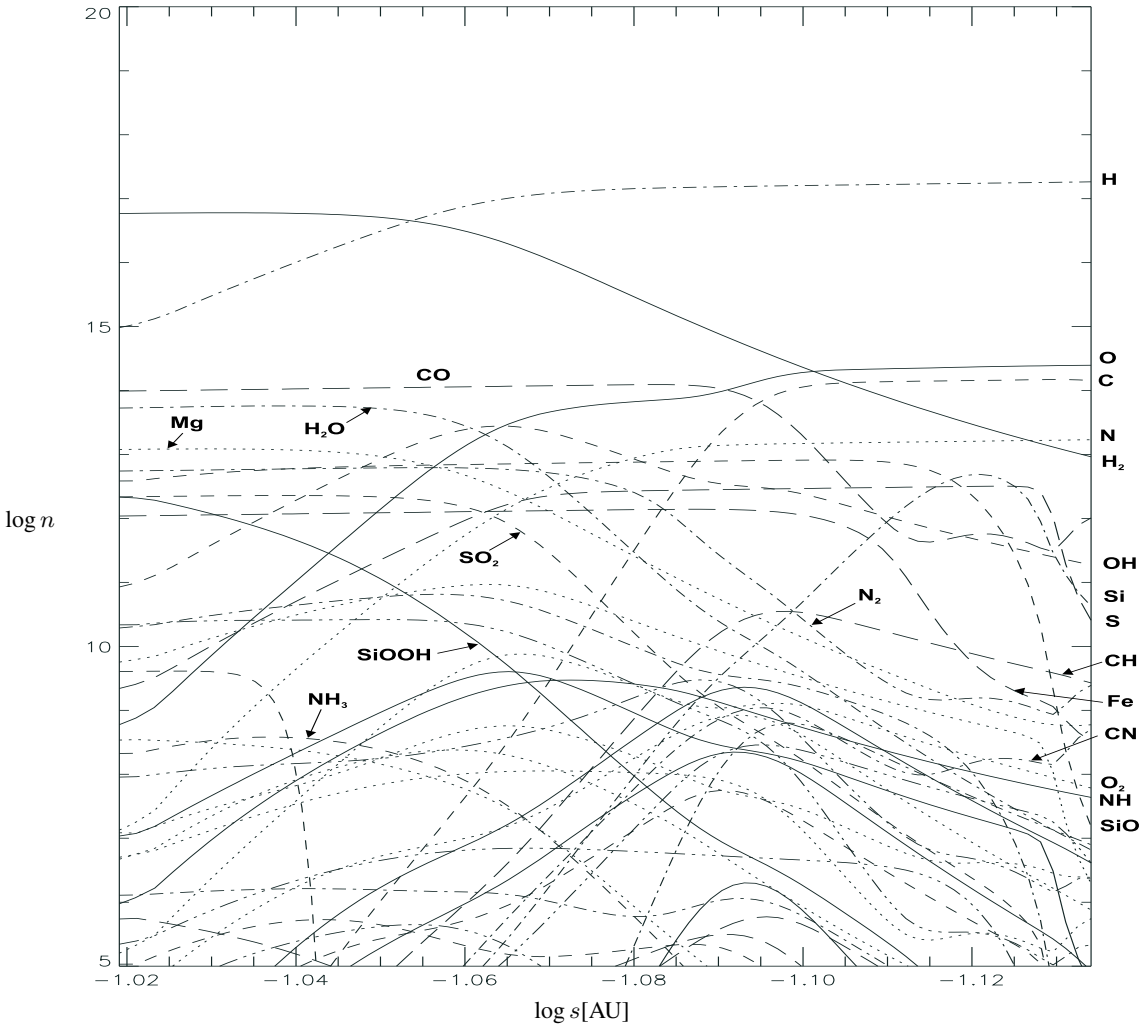

Fig. 6. Particle densities of neutral species in the innermost regions of the accretion disk.

processes provide a possibility to avoid this reaction and to produce high amounts of cyanide even at low temperatures.

In Paper II, we found that very high amounts of methane and some other hydrocarbons are formed in the region of the actual position of the Earth as a consequence of the carbon oxidation by OH. We see now, that we have also high amounts of ammonia and cyanide exactly in the same region (see Fig. 9) as a consequence of the N_2 destruction by ionisation processes due to cosmic rays and radio-nuclides.

NH_3 and HCN both disappear at about 0.8 AU ($\approx$1 300 K), where the olivine particles begin to be thermally dissociated. This injects besides others free O atoms into the gas phase which forms OH. NH_3 reacts with the newly formed OH

$$NH_3 + OH \longrightarrow NH_2 + H_2O\,, \tag{68}$$

and HCN reacts with the oxygen atoms

$$HCN + O \longrightarrow CO + NH\,. \tag{69}$$

NO reaches a high abundance at about 1.6 AU. It forms when NH reacts with water to form HNO

$$NH + H_2O \longrightarrow HNO + H_2\,. \tag{70}$$

HNO then reacts with the molecular hydrogen to form NO

$$HNO + H_2 \longrightarrow NO + H\,. \tag{71}$$

In the innermost part of the disk (see Fig. 6), the NH_i compounds react to N_2 according to the backward reactions of the reaction chain (67). Some molecules like HCN, NO and CN are produced in this region anewed. The pathway to HCN has been explained above. NO forms according to the reactions (70) and (71) and CN is produced by a reaction between N_2 and the free carbon atoms

$$N_2 + C \longleftrightarrow CN + N\,. \tag{72}$$

All these compounds disappear again at a somewhat higher temperature and are rapidly converted into N_2. HCN and CN are destroyed in the following reactions

$$HCN \overset{+OH}{\longleftrightarrow} CN \overset{+N}{\longleftrightarrow} N_2 \tag{73}$$

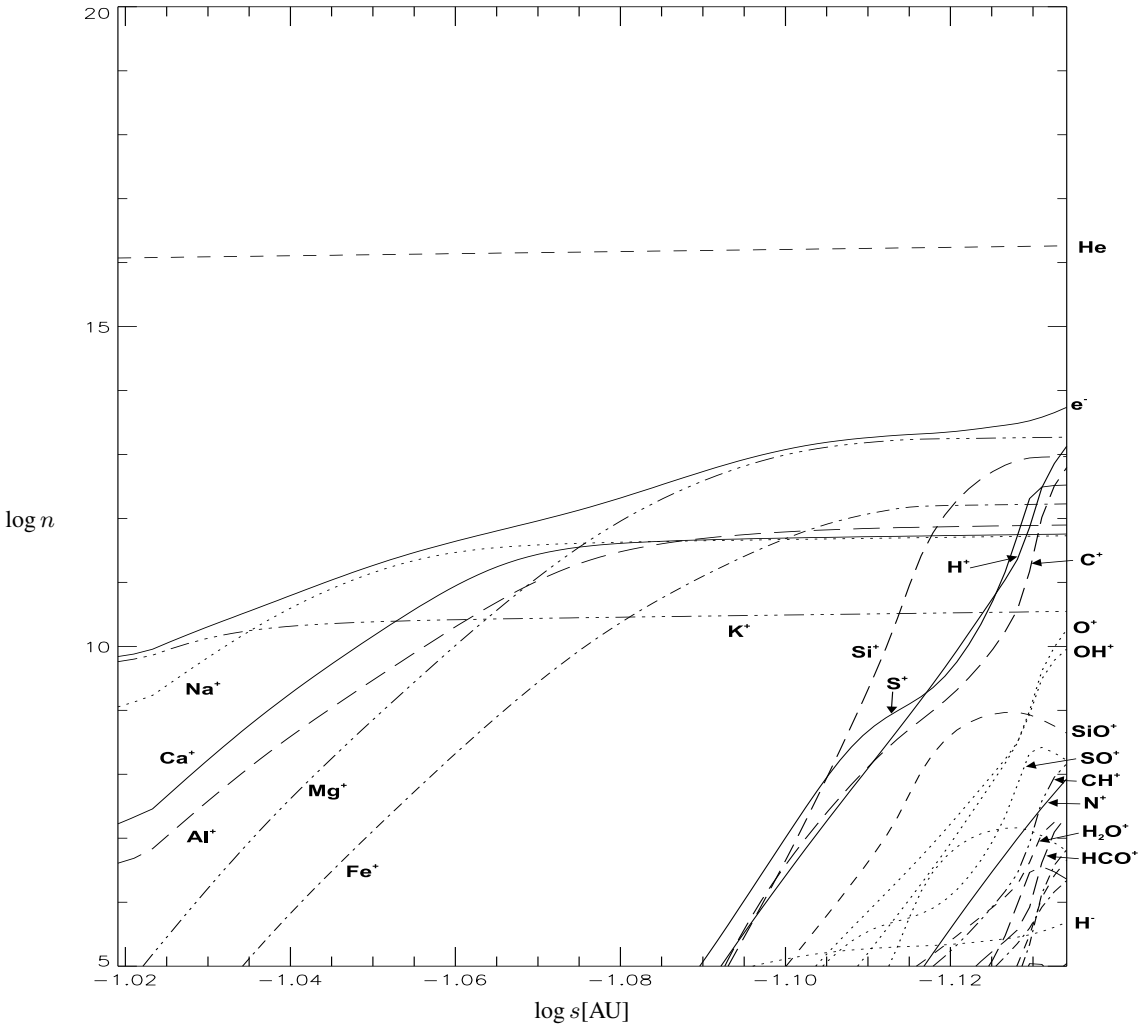

Fig. 7. Particle densities of ions in the innermost regions of the accretion disk.

and NO reacts with the free N atoms

$$\mathrm{NO + N \longleftrightarrow N_2 + O}\,. \tag{74}$$

Finally, at very high temperature, the molecular nitrogen is destroyed by collisional dissociation with H and H_2

$$\mathrm{N_2 + H \longrightarrow N + N + H} \tag{75}$$

$$\mathrm{N_2 + H_2 \longrightarrow N + N + H_2}\,. \tag{76}$$

$$\tag{77}$$

In the vicinity of the disk center only free nitrogen atoms remain.

6.3. The ion chemistry close to the central star

Fig. 6 shows that a lot of ions are formed at a distance of $\approx$0.09 AU ($T \approx$2 500 K) very close to the central star. Since this region is likely to be located already within the boundary layer between the disk and the star, where our simple disk model is no longer applicable, the results for this region are probably not realistic for real accretion disks.

We have already mentioned in Sect. 6.1 that the photoionisation processes become very important close to the central star. In order for such processes to occur, activation energy barriers corresponding to atomic ionisation energies from $\approx$50 000 K to $\approx$150 000 K have to be overcome. The heavy ions Mg^+, K^+, Na^+, Ca^+ and Al^+ have quite low ionisation energies and these ions appear at once as the corresponding atoms are injected into the gas phase during the silicate dust destruction at about 1 800 K. Small amounts of H^- and Fe^+ are formed already prior to this (Fe is already formed in the destruction of troilite). As the temperature becomes higher, the densities of these ions increase. At about 0.08 AU ($T \approx$4 000 K) the ions Si^+, S^+, H^+, C^+, O^+ and small amounts of N^+ are formed. The physical conditions prevailing there and the composition of the disk matter in this region corresponds to that of a cool stellar atmosphere.

7. Conclusions

We have calculated the gas phase chemistry in a stationary protoplanetary accretion disk including (i) the dust destruction and

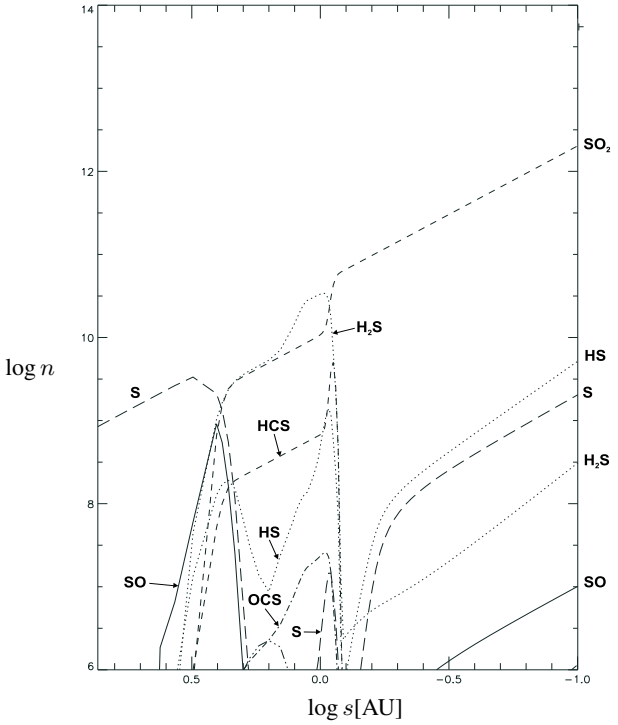

Fig. 8. Sulfur bearing species in the region of the terrestrial planets.

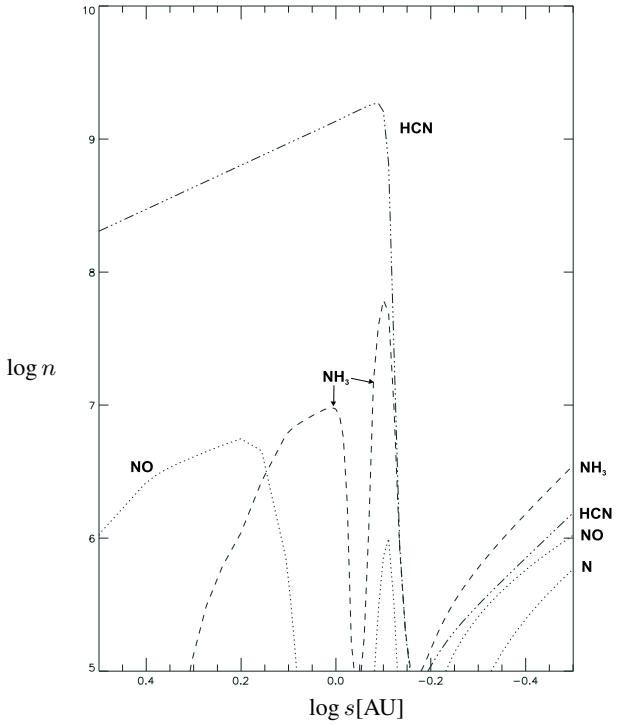

Fig. 9. Nitrogen bearing species in the region of the terrestrial planets.

their follow-up processes in the gas phase, including (ii) the ionization by cosmic rays and the unstable radio-nuclides ^{26}Al and ^{60}Fe, and including (iii) photoionisation by the local radiation field inside the disk (in LTE approximation). We have determined the chemical composition of a gas parcel in a comoving frame by solving a large (about 160 differential equations coupled with more than 1200 chemical reactions) and very stiff system of differential equations. Additional algebraic equations are coupled with the equations for the chemistry to correctly account for the coupling between temperature, opacity and the structure of the disk at one hand and the chemistry on the other hand (Sect. 3) .

Three dust components are assumed to be present in the disk (Sect. 3): silicate dust (olivine Mg_2SiO_4), carbon dust (graphite) and troilite (FeS). These grains have been supposed to be coated by distinct layers of CO and water ices, which vapourise once the appropriate temperatures are reached. The dust grains sublimate (olivine and troilite) or are destroyed by oxidation reactions (carbon). As in Paper II the gas opacity has been approximated by a set of analytical expressions (Sect. 5).

An important result of this work is the finding of high amounts of ammonia and cyanide at the actual location of the terrestrial planets (Sect. 6). The appearance of NH_3 and HCN is a direct consequence of the ionization processes, which provide a mean to destroy molecular nitrogen, making N atoms available for further chemical processes. The intensity of the ionisation processes decides wether or not large amounts of ammonia and cyanide do appear.

Another important result is the formation of quite high amounts of CS in the outer region of the disk. This molecule has been observed in the parent molecular cloud core and in circumstellar disks. As in the case of NH_3 and HCN the formation of CS is due to the ionisation processes, which strongly modify the sulfur chemistry, especially in the outer parts of the disk.

We have not discussed the implications of the ionisation processes for the electrical conductivity of the disk material and its consequences for the disk evolution, though this is probably very important (e.g. Gammie 1996), since our present model program does not consider charged grains and a distribution of grain sizes. Dust grains are important sinks for gas phase electrons, especially if there is a large population of small grains (e.g. Nishi et al. 1991). Such effects will be discussed in a forthcoming paper.

Acknowledgements. This work has been supported by the Deutsche Forschungsgemeinschaft (DFG), Sonderforschungsbereich 359 C "Reaktive Strömungen, Diffusion und Transport".

Appendix A: absorption of γ-rays in the accretion disk

In this Appendix we give a crude estimate of the conversion of the energy of γ-rays into energetic electrons. The γ-rays emitted during the decay of extinct radio-nuclides have energies of the order of $0.1 \ldots 2\,\mathrm{MeV}$ (cf. Table 3). The dominating interaction process with matter in this energy range is Compton scattering at electrons. By this process, part of the energy of the photon is transferred to the recoil electron. Since the electrons are bound in atoms, each Compton scattering event pro-

duces a recoil electron *and* an ion. At somewhat higher energy pair creation dominates, but this process has a negligible small cross section below 2 MeV. For γ energies below ≈ 50 keV the cross section of the lighter metals rapidly increases with decreasing photon energy and becomes very large as compared to the Compton scattering process (e.g. Heitler 1954). Hence the γ-rays from the nuclear decays undergo a series of Compton scatterings which reduce their average energy until their energy falls well below ≈ 0.1 MeV and they are photo-absorbed then by the light metals. By this mechanism the energy of the γ's is converted into energetic electrons. These electrons then create numerous ions by collisional ionisation of atoms and molecules during their stopping process. The ionisation by the energetic recoil electrons is more important for the ionisation of the matter than the ionisation of atoms by Compton scattering.

Let $E_\gamma = h\nu$ be the energy of the γ-quantum. Define

$$\epsilon = h\nu/m_\mathrm{e}c^2 \tag{A1}$$

and

$$\eta = E_\mathrm{e}/m_\mathrm{e}c^2 \tag{A2}$$

where m_e ist the electron rest mass and E_e the energy of the recoil electron. The frequency ratio of the γ-quantum before and after Compton scattering is

$$\frac{\nu'}{\nu} = \frac{1}{1+\epsilon(1-\cos\theta_\gamma)}\,, \tag{A3}$$

where θ_γ is the scattering angle of the γ-quantum. The differential cross section for scattering of unpolarised γ's is given by the Klein-Nishina formula

$$d\sigma = \frac{1}{2}r_0^2\,d\Omega\,\left(\frac{\nu'}{\nu}\right)^2\left(\frac{\nu}{\nu'}+\frac{\nu'}{\nu}-\sin^2\theta_\gamma\right) \tag{A4}$$

(Heitler 1954). r_0 is the classical electron radius. The energy of the recoil electron is

$$\eta = \epsilon^2\frac{1-\cos\theta_\gamma}{1+\epsilon(1-\cos\theta_\gamma)}\,. \tag{A5}$$

Solving this for $\cos\theta_\gamma$ yields

$$\mu = \cos\theta_\gamma = 1-\frac{\eta}{\epsilon(\epsilon-\eta)} \tag{A6}$$

and with (A3) and (A4) we obtain for the differential cross section per unit energy of the recoil electron

$$\frac{\mathrm{d}\sigma}{\mathrm{d}\eta} = \frac{\pi r_0^2}{\epsilon^2}\,\left(\frac{\epsilon}{\epsilon-\eta}-\frac{\eta}{\epsilon}+\mu^2\right) \tag{A7}$$

The maximum allowed value of η follows from (A6) and the condition $\mu > -1$ as

$$\eta < \frac{2\epsilon^2}{2\epsilon+1} = \eta_m\,. \tag{A8}$$

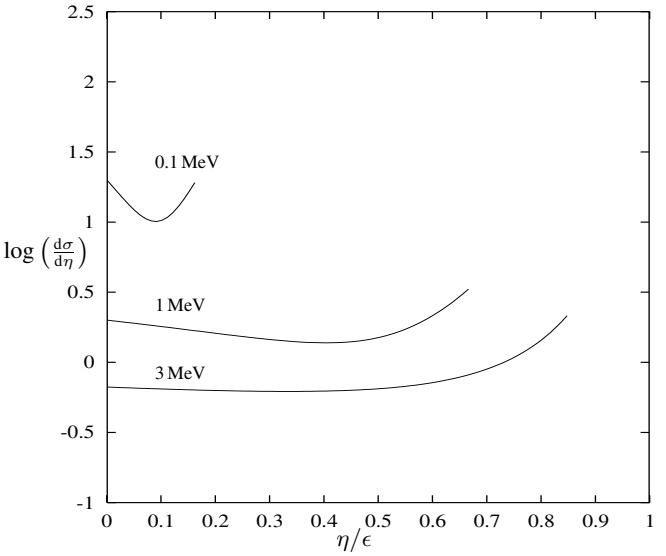

Fig. 10. Differential cross section (in units of πr_0^2) for generation of recoil electrons with energy η for three different γ energies.

The energy distribution of the recoil electrons is shown in Fig. 10. The average energy of these electrons is

$$\langle\eta\rangle = \int_0^{\eta_m} d\eta\,\eta\,\frac{\mathrm{d}\sigma}{\mathrm{d}\eta}\;/\;\int_0^{\eta_m} d\eta\,\frac{\mathrm{d}\sigma}{\mathrm{d}\eta}\,. \tag{A9}$$

For a rough estimation of $\langle\eta\rangle$ we simply put $d\sigma/d\eta$ equal to its limit at $\eta \to 0$ (cf. Fig. 10) and obtain

$$\langle\eta\rangle \approx \frac{\eta_m}{2} = \frac{\epsilon^2}{2\epsilon+1}\,. \tag{A10}$$

The average energy of the γ-particle after the scattering event is $\langle\epsilon\rangle = \epsilon - \langle\eta\rangle$. The change of the average energy of the γ-particles per scattering event then approximately is given by

$$\frac{\Delta\langle\epsilon\rangle}{\Delta N} = -\frac{\langle\epsilon\rangle^2}{2\langle\epsilon\rangle+1}\,.$$

This can be interpreted as a differential equation for the change of the average energies of the γ's with the number N of scatterings. It follows

$$N = \ln\frac{\langle\epsilon\rangle_0}{\langle\epsilon\rangle}+\frac{1}{\langle\epsilon\rangle}\,\left(1-\frac{\langle\epsilon\rangle}{\langle\epsilon\rangle_0}\right)\,. \tag{A11}$$

This N is the average number of scattering events required to reduce the initial energy $\langle\epsilon\rangle_0$ of the γ's to the final energy $\langle\epsilon\rangle$.

In order to reduce the energy of a 2 MeV photon to 0.05 MeV on the average 13 Compton scatterings are required. For a 0.5 MeV photons we require ≈ 11 scatterings and for a 0.1 MeV photon ≈ 6 scatterings. Thus, usually of the order of 10 or less scattering events are required to reduce the γ energy of the extinct radio nuclides to energies of less than 50 keV. The γ particles then have lost nearly all of their initial energy which is transferred to energetic recoil electrons. These electrons then

ionise the matter during the course of their stopping. The γ particles with energy less than 50 keV eventually are absorbed by the lighter metals or part of them may diffuse out of the accretion disk. The further fate of these quanta is of no special interest with respect to the calculation of the ionisation rate in the accretion disk since they carry only a small fraction of their initial energy, which can be neglected.

References

Anders, E., Grevesse, N., 1989, Geochimica et Cosmochimica Acta 53, 197

Bauer, I., 1994, Numerische Behandlung Differentiell-Algebraischer Gleichungen mit Anwendungen in der Chemie, Master's thesis, Universität Augsburg

Bauer, I., Finocchi, F., Duschl, W.J., Gail, H.-P., Schlöder, J.P., 1997, A&A, 317, 273 (Paper I)

Baulch, D.L., Cobos, C.J., Cox, R.A. et al., 1992, Journal of physical and chemical reference data 21, 411

Beckwith S.V.W., Sargent A.I., 1993, in Protostars and Planets III, E.H. Levy and J.I. Lunine Eds., University of Arizona Press, Tuscon, p. 521

Bell, K.R., Lin, D.N.C., 1994, ApJ 427, 987

Bell K.R., Lin D.N.C., Hartmann L.W., Kenyon S.J., 1995, ApJ 444, 376

Birck J.L., Lugmair G.W., 1988, Earth Planet. Sci. Lett 90, 131

Blake, G.A., van Dischoeck, E.F., Sargent, A.I., 1992, ApJ 391, L99

Bleser, G., 1986, Eine effiziente Ordnungs- und Schrittweitensteuerung unter Verwendung von Fehlerformeln für variable Gitter und ihre Realisierung im Mehrschrittverfahren vom BDF-Typ, Master's Thesis, Universität Bonn

Britten, J.A., Tong, J., Westbrook, C.K., 1990, Twenty–Third Symposium (International) on Combustion/The Combustion Institute, 195

Cameron, A.G.W., 1988, AR&A 26, 441

Cameron A.G.W., 1993, in Protostars and Planets III, E.H. Levy and J.I. Lunine Eds., Univ. of Arizona Press, Tucson, p. 47

Cannizzo J.K., 1993, in: Accretion disks in compact stellar systems, J.C. Wheeler Ed., World Scientific Publ. Comp., Singapore etc., p. 6

Cassen P., 1994, Icarus 112, 405

Cecchi-Pestellini C., Aiello S., 1992, MNRAS 258, 125

Clayton D., 1968, Principles of stellar evolution and nucleosynthesis, McGraw-Hill, New York etc.

Consolmagno G.J., Jokipii J.R., 1976, Moon and Planets 19, 120

Cowie L.L., Songaila A., 1986, ARA&A 24, 499

Dalgarno A., Griffing G.W., 1958, Proc. Roy. Soc. A248, 415

Dalgarno A., McCray R.A., 1972, ARA&A 10, 375

del Rio E., von Ballmoos P., Bennet K. et al., 1996, A&A 315, 237

Dolginov A.Z., Stepinski, T.F., 1994, Astrophysical J., 427, 377

Draine, B.T., Lee, H.M., 1984, ApJ 285, 89

Draine, B.T., 1985, ApJS 57, 587

Dutrey A., Guilloteau S., Guérin M., 1997, A&A (submitted)

Duschl W.J., Gail H.-P., Tscharnuter W.M., 1996, A&A 312, 624

Eich, E., 1987, Numerische Behandlung semi-expliziter differentiellalgebraischer Gleichungssysteme vom Index 1 mit BDF-Verfahren, Master's Thesis, Universität Bonn

Finocchi, F., Gail, H.-P., Duschl, W.J., 1997, A&A, (in press) (Paper II)

Fish R.A., Goles G.G., Anders E., 1960, ApJ 132, 243

Gammie C., 1996, ApJ 457, 355

Glassgold A.E., 1995, ApJ 438, L111

Grevesse, N., Noels, A., 1993, Cosmic Abundances of the Elements, in Origin and Evolution of the Elements, N. Prantzos, E. Vangioni-Flam and M. Cassé, Cambridge University Press, p. 14

Grossman L., 1972, Geochimica et Cosmochimica Acta 36, 597

Harper Jr. L.H., 1996, ApJ 466, 1026

Hartmann L., Kenyon S.J., 1996, ARA&A 34, 207

Heitler W., 1954, The quantum theory of radiation, 3rd ed., Oxford, At the Clarendon Press

Herbig G.H., 1977, ApJ 217, 693

Jenkins E.B., 1989, in: Interstellar Dust, eds. L.J. Allamandola and A.G.G.M. Thielens, IAU Symposium No. 135, Kluwer, Dordrecht, p. 23

Kutschera W. et al., 1984, Nucl. Inst. Meth. Phys. Res. Sect. B 5, 430

Landini M., Monsignori Fossi B.C., 1990, A&AS 82, 229

Lee T., Papanastassiou D.A., Wasserburg G.J., 1977, ApJ 211, L107

Lepp S., 1992, in: Astrochemistry of Cosmic Phenomena, IAU Symp. 150, Kluwer, Dordrecht etc., p. 471

Lide R.D., 1995, CRC Handbook of Chemistry and Physics, 76th ed., CRC Press, Boca Raton etc.

Lin D.N.C., Papaloizou J., 1995. in Protostars and Planets II, D.C. Black and M.S. Matthews Ed., Univ. of Arizona Press, Tucson, p. 981

Lugmair G.W., Galer S.J.G., 1992, Geochimica et Cosmochimica Acta 56, 1673

Mahoney W.A., Ling J.C., Wheaton W.A., Jacobson A.S., 1984, ApJ 286, 578

Mathis, J.S., Rumpl, W., Nordsieck, K.H., 1977, ApJ 217, 425

Millar, T.J., Rawlings, J.M.C., Benett, A., Brown, P.D., Charnley, S.B., 1991, A& AS 87, 585

Millar T.J., Farquhar P.R.A., Willacy K., 1997, A&AS 121, 139

Mitchell, G.F., 1984, ApJS 54, 81

Neufeld D.A., Hollenbach, D.J., 1994, ApJ 428, 170

Nishi R., Nakano T., Umebayashi, T., 1991, ApJ 368, 181

Ohashi N., Kawabe R., Hayashi M., Ishiguro H., 1991, ApJ 102, 2054

Pollack J.B., Hollenbach D., Beckwith S. et al., 1994, ApJ 421, 615

Prasad S.S., Tarafdar S.P., 1983, ApJ 267, 603

Ramaty R., Lingenfelter R.E., 1977, ApJ 213, L5

Romani, P.N., 1996, Icarus 122, 233

Ruden, S.P., Pollack, J.B., 1991, ApJ 375, 740

Shukolyukov A., Lugmair G.W., 1993, Science 259, 1138

Spitzer L., Tomasko M.G., 1968, ApJ 152, 971

Swindle T.D., 1993, in Protostars and Planets III, E.H. Levy and J.I. Lunine Eds., Univ. of Arizona Press, Tucson, p. 897

Umebayashi, T., Nakano, T., 1981, Publ. Astron. Soc. Japan 33, 617

van Langenvelde, H.J., van Dishoeck, E.F., Blake, G.A., 1994, ApJ 425, L45

Wasserburg G.J., 1985, in Protostars and Planets II, D.C. Black and M.S. Matthews Eds., Univ. of Arizona Press, Tucson, p. 703

Wasserburg G.J., Papanastassiou D.A., 1982, in Essays in Nuclear Astrophysics, C.A. Barnes, D.D. Claton, and D.N. Schramm eds., Cambridge University Press, Cambridge etc., p.77

Wasserburg G.J., Busso M., Gallino R., Raiteri C.M., 1994, ApJ 424, 412

Weidenschilling S.J., Cuzzi J.N., 1993, in Protostars and Planets III, E.H. Levy and J.I. Lunine Eds., Univ. of Arizona Press, Tucson, p.1031

This article was processed by the author using Springer-Verlag LaTeX A&A style file *L-AA* version 3.